WORKING PAPERS

N° 1721

February 2026

"Capital Sunk, Emissions Locked: The Economics of Energy Transitions under Carbon Constraints"

Michel Moreaux, Jean-Pierre Amigues
and Manh-Hung Nguyen

Toulouse School of Economics

Capital Sunk, Emissions Locked: The Economics of Energy Transitions under Carbon Constraints*

Michel Moreaux† Jean-Pierre Amigues‡ Manh-Hung Nguyen§

February 9, 2026

Abstract

Optimal energy transitions are characterized in an economy where fossil energy requires dedicated conversion capital that is costly to reverse and where cumulative emissions are capped by an exogenous carbon budget. Short-run complementarity between fossil inputs and sector-specific capital interacts with intertemporal scarcity of the remaining budget. The optimal path typically selects an expansion regime, a production plateau, a decline regime, and a post-fossil steady state. The plateau is pinned down by the need to operate in order to amortize sunk conversion capital while the shadow value of remaining emissions rises over time. These forces generate non-monotone useful-energy prices and deliver sharp conditions under which dedicated fossil capital becomes stranded.

Calibrated to global energy data, the baseline features a plateau of about 42 years accounting for 48% of cumulative emissions. Delaying policy by 20 years lowers welfare by 1.8% and strands $287 bn in assets; a 40-year delay lowers welfare by 4.3% and strands $532 bn. When explicit carbon taxation is infeasible, quantity instruments approximate the tax allocation in the calibration: a capacity cap and an investment ban deliver welfare losses of 0.8% and 1.2%, respectively.

Keywords: Carbon constraint, Nonrenewable resources, Renewable resources, Energy transition, Hotelling rule.

JEL Classification: E22, Q00, Q32, Q43, Q54.

*This project began under the impetus and strong guidance of Michel Moreaux. Michel passed away in November 2021, and we miss him deeply. The authors acknowledge funding from the French National Research Agency (ANR) under the Investment for the Future (Investissements d'Avenir) program, grant ANR-17-EURE-0010. Corresponding author: M. H. Nguyen (*manh-hung.nguyen@tse-fr.eu*)

†Toulouse School of Economics, Université de Toulouse Capitole, Toulouse, France.

‡Toulouse School of Economics, Université de Toulouse Capitole, Toulouse, France.

§Toulouse School of Economics, INRAE, Université de Toulouse Capitole, Toulouse, France.

1 Introduction

Fossil fuel prices and extraction paths have long posed a challenge for the canonical Hotelling benchmark (Hotelling, 1931). Even after allowing for technological progress and exploration dynamics, recent empirical work finds persistent departures from Hotelling-style predictions for oil, gas, and coal (Anderson et al., 2018; Gaudet and Lasserre, 2022). Using more than a century of data across multiple commodities, Stürmer (2018) documents that real resource prices have more often trended downward than upward, and attributes this pattern to sustained technological progress that compresses scarcity rents.

A natural mechanism for such departures is the capital intensity of extraction. When production requires large, lumpy, and partially irreversible investments, firms' intertemporal choices can differ sharply from those in frictionless exhaustible-resource models, and equilibrium price and quantity dynamics need not resemble Hotelling-type paths; see, e.g., (Puu, 1977; Crémer, 1979; Campbell, 1980; Lasserre, 1982, 1985a,b; Cairns and Lasserre, 1986; Olsen, 1989; Cairns and Lasserre, 1991; Lozada, 1993; Cairns, 1998, 2001; Holland, 2003a). A related literature studies how fixed and setup costs shape competitive equilibria in resource markets (Hartwick et al., 1986; Holland, 2003b; Vu and Im, 2011; Bommier et al., 2018).[1] More recent work emphasizes that irreversibility interacts with policy uncertainty: when capital is sunk, private and political incentives may tilt toward delay even under substantial increases in carbon prices (Coulomb and Henriet, 2018). In the same vein, Lemoine and Rudik (2017) shows that uncertainty about climate damages and technological change creates option values that slow both mitigation and adaptation.

Even when Hotelling-type models are amended to incorporate investment costs, they say little about how scarcity in primary resources translates into prices of downstream energy services. In the transformation chain from underground energy to final consumption, most capital is not located in extraction but in conversion and infrastructure systems. Oil, for example, must be refined and often further converted into electricity or hydrogen, then combined with vehicles and transport networks to deliver useful mechanical energy.[2] As renewable energy penetration increases, downstream capital requirements become even more prominent, particularly through grid infrastructure needed to manage intermittency and reliability (Joskow, 2011; Hirth, 2015; Millstein et al., 2021).

Much of this downstream capital is highly specific to fossil fuel use and cannot be redeployed to clean energy without significant cost. This specificity has gained renewed attention following the Paris Agreement and subsequent climate commitments. Pfeiffer

[1] A broader notion of capital would include both R&D and exploration expenditures.

[2] See Fouquet (2008) for a historical review of useful energy prices. Kander et al. (2013) and Stern (2011) document more recent developments.

et al. (2016) show that operating existing fossil infrastructure through its planned lifetime would exhaust remaining carbon budgets consistent with limiting warming to 1.5°C or 2°C, creating a tension between amortizing sunk investments and meeting climate targets. This tension is reflected in a striking empirical pattern: despite solar photovoltaic costs falling by more than 60% between 2010 and 2022 (IRENA, 2023), global coal-fired capacity continued to expand over the same period, even as carbon prices remained low and heterogeneous (Table 1). This persistence contrasts sharply with models predicting smooth technological substitution in response to relative price changes.

Table 1: **The Fossil Lock-In Paradox: Divergent Global Trends**

Year	Coal Capacity (GW)	Carbon Price (USD/tCO$_2$)	Solar LCOE (USD/kWh)
2010	1,879	∼9	0.138
2015	2,010	∼12	0.087
2020	2,145	∼21	0.060
2022	2,167	∼25	0.053

Note: Coal capacity aggregates global coal-fired power generation. Carbon prices are approximate emissions-weighted averages across jurisdictions with carbon taxes or emissions trading systems; coverage grew from roughly 5% of global emissions in 2010 to about 23% by 2022, so cross-year comparisons should be treated with caution. Solar LCOE denotes the global weighted-average levelized cost of electricity for utility-scale photovoltaic installations. Coal capacity data are from Global Energy Monitor (2025). Carbon price data are from the World Bank Carbon Pricing Dashboard (World Bank, 2024). Solar cost estimates are from the International Renewable Energy Agency (IRENA, 2023).

Capital specificity matters most when climate policy is framed in terms of a cumulative emissions constraint. We assume a finite carbon budget consistent with long-run temperature stabilization goals, as articulated in the Paris Agreement. Recent IPCC assessments place the remaining budget at roughly 500 GtCO$_2$ for a 50% chance of limiting warming to 1.5°C, and about 1,150 GtCO$_2$ for 1.75°C (IPCC, 2021, 2022). Under such a constraint, carbon is scarce in an intertemporal sense: the key restriction is cumulative emissions, not contemporaneous flows alone.

A growing literature models the carbon budget as an exhaustible resource. Golosov et al. (2014) show that finite atmospheric capacity generates positive and rising carbon rents in dynamic general equilibrium, while Hassler and Krusell (2018) show that optimal carbon taxes can rise faster than the Hotelling rate when clean innovation features learning-by-doing. Related work studies the implications of cumulative constraints for stranded assets and price dynamics (Barbier and Burgess, 2017; van der Ploeg and Rezai, 2020; Dietz and Venmans, 2019). Integrated assessment models with capital vintages and retrofit costs imply stranded assets on the order of trillions of dollars under ambitious scenarios (Bauer et al., 2015, 2023; Luderer et al., 2022; Kriegler et al., 2023).

We develop a tractable model of the energy transition in which (i) fossil energy requires dedicated conversion capital that is irreversible once installed and (ii) cumulative emissions are constrained by an exogenous carbon budget. The planner internalizes both the scarcity rent on the remaining carbon budget and the quasi-rents on fossil-specific capital. Their interaction can generate an extended interval in which fossil capacity is optimally held fixed even as renewables expand and the carbon price continues to rise. This mechanism rationalizes the persistence of fossil capacity observed in practice and delivers transparent conditions under which fossil-related capital becomes stranded along the transition path.

We characterize the optimal transition analytically and then quantify transition dynamics and policy costs in a calibrated version of the model.

We apply the framework to an economy with two energy sources: a renewable technology (solar) and a non-renewable resource (coal). The analysis departs from standard transition models by making explicit the dedicated capital required to convert coal into usable energy services. In contrast to the smooth substitutability typically assumed in the directed technical change literature (Acemoglu et al., 2012; Hassler and Krusell, 2018), we impose strong short-run complementarity between coal and fossil-specific capital. This complementarity implies a transition with distinct phases, including a plateau during which fossil-based energy production remains constant as the economy amortizes sunk conversion capital while the shadow value of the remaining carbon budget rises over time.

Embedding capital–resource complementarity in a setting with a cumulative emissions constraint links the Hotelling logic for exhaustible resources to the carbon-budget interpretation of climate policy. The key implication is that declining renewable costs need not translate into an immediate contraction of fossil output when fossil use is tied to dedicated conversion capital. This mechanism helps rationalize the pattern in Table 1, where coal generation remains elevated despite rapid cost declines in renewables.

Most analyses of optimal carbon pricing emphasize the scarcity rent on cumulative emissions—the shadow value of the remaining carbon budget (Golosov et al., 2014; Nordhaus, 2017; Lemoine and Traeger, 2014; Gollier, 2024). Our framework introduces a second scarcity margin: retiring sector-specific productive capital before it is fully amortized. When the shadow value of the carbon budget rises while fossil capital is quasi-fixed, the interaction between carbon scarcity and capital irreversibility generates transition dynamics that are absent under frictionless substitution across energy technologies.

For tractability, we consider an economy with two energy sources. Coal is an exhaustible resource that must be combined with sector-specific capital to produce usable energy. Solar is a renewable flow produced with non-dedicated capital; its marginal cost is increasing in scale (e.g., due to site quality and integration costs) but it does not in-

herit the same lock-in from fossil-specific infrastructure. We abstract from intermittency, storage, grid constraints, and endogenous directed technical change in order to isolate a single mechanism: irreversible, sector-specific capital creates path dependence in the optimal transition when cumulative emissions are constrained.

Coal extraction is assumed to have constant marginal cost and no fixed installation costs. In our setting, the relevant exhaustible stock is the remaining carbon budget rather than the coal deposit itself. Accordingly, the shadow value of the remaining carbon budget satisfies a Hotelling condition, and the effective marginal cost of coal use rises over time through the carbon price component. Conversion of coal into usable energy, by contrast, requires a stock of sector-specific capital. We represent conversion with a three-input Leontief technology that combines coal, capital services, and a supplementary input (e.g., labor), which imposes strict short-run complementarity between coal and the dedicated capital.

Complementarity in the short run does not preclude substitution over time. For a given installed capital stock, coal use is governed by utilization—the duration and intensity with which the capital is operated—whereas cumulative processing is determined by when that capital is accumulated and when it is ultimately retired. Through this channel, capital dynamics pin down the time profile of coal use and hence the associated path of carbon emissions. Conversely, depletion of the carbon budget feeds back into optimal investment and scrapping decisions for fossil-specific capital. The interaction between carbon scarcity and capital irreversibility therefore becomes a first-order determinant of transition dynamics.

We model solar more sparingly. Solar is a renewable flow produced without fossil-specific capital lock-in; its marginal cost is increasing in scale, but it does not require a dedicated conversion stock analogous to that in the coal sector. Under standard assumptions on preferences, convex adjustment costs for investment, and constant per-unit maintenance costs, the optimal transition can be described as a sequence of four phases: an initial period in which coal-based energy expands while solar contracts; a plateau during which coal output is held at its maximum; a phase in which the tightening carbon constraint induces declining coal production alongside expanding solar; and, finally, a terminal phase in which energy production is fully renewable.

Relative to standard models that deliver a symmetric "peak oil" profile, irreversible investment in fossil infrastructure produces a prolonged plateau. Dedicated capital must operate long enough to recover its upfront cost even as the shadow value of the remaining carbon budget rises. This mechanism aligns with the persistence of coal generation observed in practice. Germany's coal phase-out, initially scheduled for 2038 and later accelerated toward 2030, was accompanied by an extended period of roughly constant generation despite rapid renewable expansion (Pahle et al., 2022). In China, coal capac-

ity has been on the order of 1,100 GW since the early 2020s even as coal's share in total generation has declined (Global Energy Monitor, 2023). In the United Kingdom, coal output remained broadly stable for nearly two decades before declining rapidly after 2010 (Speirs et al., 2015).

During the first three phases of the transition, aggregate useful energy, the sum of coal and solar-based output, exceeds the level delivered in the terminal all-renewable phase. The price of useful energy is non-monotone: it declines during the initial build-out of coal-specific capital, is flat over the production plateau, and rises during the coal phase-out, eventually converging back to its initial level. By contrast, the effective marginal cost of coal use, the marginal extraction cost plus the carbon price, moves monotonically. With constant marginal extraction cost, its time profile is pinned down by the carbon price, which increases at the planner's discount rate along the optimal depletion of the carbon budget. In our calibration, the carbon price rises from about $\$22/\text{tCO}_2$ initially to above $\$200/\text{tCO}_2$ at budget exhaustion, a range in line with recent empirical SCC estimates (Rennert et al., 2022).

The wedge between these price paths reflects shifting scarcity from fossil-specific capital to the carbon budget. Early in the transition, the shadow value of coal-specific capital falls as capacity accumulates, and this decline more than offsets the rising carbon price, generating a negative comovement between the price of useful energy and the effective marginal cost of coal. Over the plateau, the two forces approximately offset, leaving the price of useful energy essentially constant. Once the shadow value of coal-specific capital is driven to zero, continued coal use entails only maintenance and the carbon price, and the price of useful energy becomes increasingly disciplined by the rising scarcity rent on the remaining carbon budget.

These dynamics reflect intertemporal substitution between two constraints—coal-specific capacity and cumulative emissions. Accordingly, the optimal transition need not feature a single, sharp emissions peak; instead it can exhibit a sustained plateau in coal-based production and associated CO_2 emissions. This source of transition inertia is distinct from political-economy mechanisms (Branger and Quirion, 2014), learning-by-doing in clean technologies (Hassler and Krusell, 2018), or option value under uncertainty (Lemoine and Rudik, 2017; Lemoine and Traeger, 2014). It arises under certainty and perfect foresight as a direct implication of irreversibility and the incentive to amortize sunk capital.

Our results speak to three policy questions that recur in current debates: how to interpret persistent fossil use during the transition, how costly delayed action can be, and how to manage the risk of stranded assets when long-run targets shift.

Persistent fossil production need not, by itself, indicate policy failure. When fossil

energy is tied to irreversible, sector-specific capital, the optimal response to a cumulative carbon constraint can include a prolonged production plateau. During this phase, renewable output expands and the carbon price rises, yet fossil capacity is held fixed to complete the amortization of sunk conversion capital.

Delaying policy implementation is costly because it induces over-accumulation of fossil-specific capital and then forces a compressed adjustment once the constraint becomes binding. In our quantitative exercises, a 20-year delay generates stranded assets of \$287 bn and a welfare loss of 1.8%, while a 40-year delay raises stranded assets to \$532 bn and the welfare loss to 4.3% (Table 4). These magnitudes put quantitative content behind precautionary arguments for earlier action, as in Lemoine and Traeger (2014).

The model also clarifies the economic origin of stranded assets and how it differs from "technological obsolescence." In our framework, stranding arises when a tighter carbon constraint renders previously built, dedicated capital unable to recover its upfront cost. For example, when the carbon budget is unexpectedly tightened at year 30, the optimal response entails immediate scrapping of 120 EJ/yr of fossil-specific capacity, valued at \$185 bn, and a welfare loss of 1.4% relative to perfect foresight under the tighter budget; these orders of magnitude are in the range reported by integrated assessment models (Luderer et al., 2022). The same logic implies a role for policies that affect how quickly renewables become competitive: learning-driven declines in renewable costs shorten the plateau by pulling forward the point at which solar displaces coal, complementing carbon pricing in accelerating the transition (Acemoglu et al., 2012).

The framework is useful for evaluating second-best policy instruments when explicit carbon taxation is politically constrained. In our calibration, quantity-based policies can approximate the first-best carbon tax closely when calibrated to the same carbon budget. A capacity cap delivers a welfare loss of 0.8% relative to the tax benchmark, and an investment ban delivers a welfare loss of 1.2% (Table 5).

The remainder of the paper is organized as follows. Section 2 presents the model. Section 3 formulates the social planner's problem and derives the associated optimality conditions. Section 4 characterizes the qualitative structure of optimal transition paths and establishes the four-phase pattern. Section 5 describes the calibration strategy and parameter choices. Section **??** reports quantitative results and policy experiments. Section 6 concludes. Technical details and proofs are provided in the appendices.

2 The model

We consider an economy producing useful energy (U.E) from either a polluting non-renewable primary energy resource (coal) or from a clean renewable resource (solar).

Coal useful energy (C.U.E) and solar useful energy (S.U.E) are perfect substitutes for the final users. We denote by q_x the instantaneous production rate of C.U.E, by q_y the instantaneous production rate of S.U.E and by q the instantaneous production rate of U.E. Under the perfect substitutability assumption $q(t) = q_x(t) + q_y(t)$, $t \geq 0$. Without useful energy storage possibilities, $q(t)$ is also the U.E consumption rate.

User surplus

Let $u(q(t))$ denote the instantaneous gross surplus of the U.E users. The function u is assumed to satisfy the below standard assumption.[3]

Assumption A. 1 *$u : \mathbb{R}_{++} \to \mathbb{R}$ is twice continuously differentiable, strictly increasing and strictly concave with $u'(0^+) = +\infty$ and $u'(\infty) = 0$.* [4]

We sometimes denote by $p(q)$ the marginal surplus function $u'(q)$, the inverse demand function, and by $q^d(p)$ the direct demand function, the inverse of $p(q)$, where p is the U.E price.

Coal U.E production

Producing U.E from coal requires capital and other inputs together with coal. We assume that the C.U.E production function is a Leontief one and without loss of generality that there is only one input other than capital and coal, hence the following Assumption A.2.

Assumption A. 2 *The C.U.E production function reads:*

$$q_x = \min\{K, v, \bar{r}x\}, \;\; K, v, x \geq 0 \text{ and } 1 > \bar{r} > 0 \;, \tag{2.1}$$

where x, K, v are respectively the coal, the capital and the other input, all measured in energy units.

The assumption $\bar{r} < 1$ means that some energy is lost in the transformation of coal into U.E. In what follows we mainly use its inverse $r = 1/\bar{r} > 1$, the quantity of coal energy required to produce one unit of U.E.[5]

[3] For any function $f(x)$ defined on $X \subseteq R$ we denote by $f(\bar{x}^+)$ and $f(\bar{x}^-), \bar{x} \in X$, respectively, the limits $\lim_{x \downarrow \bar{x}} f(x)$ and $\lim_{x \uparrow \bar{x}} f(x)$ when such limits exist.

[4] Admittedly we need only that $u'(0^+)$ be "sufficiently" high.

[5] It is well known that the energy is constant. Thus by energy loss we mean that some part of the chemical energy of coal is transformed into energy improving the surplus of the final users, the remaining being mostly dissipated in useless heat.

We denote by c_v the unitary cost of the input v, assumed to be constant through time. The capital K is dedicated to the production of C.U.E without valuable use outside the C.U.E industry and requires a unitary maintenance cost m assumed to be constant through time. This capital dies by lack of maintenance and cost-free scrapping. Let $k(t)$ be the production rate of new capital, then absent any "abrupt" reduction of the installed capacity $K(t)$, the capital stock dynamics satisfies the following condition:[6]

$$\dot{K}(t) = k(t) - \delta(t)K(t), \quad \delta(t) \geq 0, \quad t > 0 \ , \tag{2.2}$$

where $\delta(t)$ is the instantaneous proportional scrapping rate.

Let $c_k(k)$ be the production cost function of new capital. This function satisfies the following standard Assumption A.3 where $c'_k(k)$ and $ac_k(k)$ denote respectively the marginal and the average cost functions.

Assumption A. 3 *$c_k : \mathbb{R}_+ \to \mathbb{R}_+$ is a twice continuously differentiable function, strictly increasing and strictly convex, with $c_k(0) = 0$ and $c'_k(0^+) = ac_k(0^+) > 0$.*

The assumption $c'_k(0^+) > 0$ means that nothing can be built without some costly input. In what follows we use the more compact notation $\underline{c'_k}$ for $c'_k(0^+)$. Time $t = 0$ is the time at which the technical knowledge required to produce useful energy from coal becomes available, that is the time of the industrial revolution (see Wrigley 1988, 2010, and 2016).

Carbon emissions and budget constraint

Let $x(t)$ be the flow of fossil fuel used at time t and $\zeta > 0$ the average carbon content of fossil fuels, measured in $GtCO_2$ per unit of x. Then the corresponding carbon emissions flow is $\zeta x(t)$. Let $B(t)$ denote the remaining allowable cumulative carbon budget, with initial condition $B(0) = B_0 > 0$. The dynamics of $B(t)$ are given by:

$$\dot{B}(t) = -\zeta x(t) = -\zeta r q_x(t) \ . \tag{2.3}$$

Although the scarcity of the non-renewable coal reserves should be accounted for, we assume that the initial coal reserves, we denote $X(0)$, satisfy $\zeta X(0) > B(0)$, so that the coal energy industry cannot deplete the coal reserves while satisfying at the same time the carbon budget constraint. Then the coal scarcity issue can be neglected and no specific scarcity rent has to be added to the opportunity cost of coal use. There is only one scarce resource in the model, the safe storage space for carbon emissions in the atmosphere. The carbon budget constraint replaces the traditional resource stock constraint and will

[6] By "abrupt" reduction at a time t we mean that $K(t^-) > K(t^+)$.

play a central role in determining the optimal trajectory of fossil fuel use and the timing of the transition to renewable energy.

To simplify, we assume that the extraction and delivery cost of fossil fuels to the C.U.E industry is linear in x, hence:

Assumption A. 4 *$c_x : \mathbb{R}_+ \to \mathbb{R}_+$ is the linear function $c_x(x) = \underline{c}_x x$, $\underline{c}_x > 0$.*

Solar U.E production

The sites devoted to the production of solar U.E are exploited by merit order that is by increasing marginal opportunity costs including the loss in net surplus generated by their allocation to the S.U.E production rather than to other net surplus generating uses, for example food production when S.U.E is biofuel. However for some S.U.E production processes the opportunity cost is nil, for example the S.U.E production via photovoltaic cells in desert land. Taking care that other costs than the pure opportunity loss must be supported, we assume, denoting by $c_y(q_y)$ the full cost of S.U.E and by $c'_y(q_y)$ and $ac_y(q_y)$ respectively the marginal and average costs, that:

Assumption A. 5 *$c_y : \mathbb{R}_+ \to \mathbb{R}_+$ is a twice continuously differentiable function, strictly increasing and strictly convex, with $c_y(0) = 0$ and $c'_y(0^+) = ac_y(0^+) > 0$.*

The rationale for $c'_y(0^+) > 0$ is the same as for $c'_k(0^+) > 0$, and we use from now the more compact notation $\underline{c}'_y$ for $c'_y(0^+)$.

When the S.U.E industry is the only supplier of U.E, then the marginal surplus $u'(q_y)$ must be equal to its marginal cost $c'_y(q_y)$. Under A.1 and A.5 the solution of $u'(q_y) = c'_y(q_y)$ is unique and strictly positive. We denote by $\tilde{q}_y$, equivalently by $\tilde{q}$, this solution and by $\tilde{p}$ the corresponding U.E price: $\tilde{p} = u'(\tilde{q})$. This is the state of the energy sector at the beginning and at the end of the fossil fuel interlude.

In order that the C.U.E production be a competitive option we must assume that its lowest marginal cost be lower than the marginal cost of the S.U.E production when S.U.E is the only supplier of U.E, hence:

Assumption A. 6 *$c_v + r\underline{c}_x + \rho\underline{c}'_k + m < c'_y(\tilde{q})$, where $\rho\underline{c}'_k$ is the rental cost of the least costly piece of C.U.E equipment valued at the social rate of discount ρ.*

The welfare W is the sum of the net surplus discounted at a social rate of discount $\rho > 0$, constant through time.

3 The social planner problem and preliminary results

The social planner determines a path $\{(q_x(t), q_y(t), k(t), \delta(t))\}_{t=0}^{\infty}$ maximizing the social welfare, that is solves the following problem (S.P):

$$\text{(S.P)} \quad \max_{q_x, q_y, k, \delta} \int_0^{\infty} \{u(q_x(t) + q_y(t)) - (c_v + r\underline{c}_x)q_x(t) - mK(t) - c_k(k(t)) - c_y(q_y(t))\}e^{-\rho t}dt \tag{3.1}$$

$$s.t. \qquad \dot{B}(t) = -\zeta r q_x(t), \ B(0) = B_0 > 0 \text{ given}, \ B(t) \geq 0 \tag{3.2}$$

$$\dot{K}(t) = k(t) - \delta(t)K(t), \ K(0) = 0, \ K(t) \geq 0 \tag{3.3}$$

$$K(t) \geq q_x(t), \ q_x(t) \geq 0, \ q_y(t) \geq 0, \ k(t) \geq 0, \ \delta(t) \geq 0. \tag{3.4}$$

3.1 Optimality conditions

For the dual variables we denote by λ's the co-state variables, by ν's the Lagrange multipliers associated with the constraints on the state variables, by γ's the multipliers associated with the constraints on the control variables, and by η the multiplier associated with the constraint involving both a state and a control variable. We denote $-\lambda_B$ the co-state associated with the state variable B in order that λ_B be positive, thus standing as the social cost of carbon.

The current-value Hamiltonian, $\mathcal{H}$, and Lagrangian, $\mathcal{L}$, read:[7]

$$\begin{aligned}\mathcal{H} &= u(q_x + q_y) - (c_v + r\underline{c}_x)q_x - mK - c_k(k) - c_y(q_y) - \lambda_B \zeta r q_x \\ &\quad + \lambda_K(k - \delta K); \\ \mathcal{L} &= \mathcal{H} + \nu_B B + \nu_K K + \eta(K - q_x) + \gamma_x q_x + \gamma_y q_y + \gamma_k k + \gamma_\delta \delta.\end{aligned}$$

[7] We drop the time argument as far as no confusion is possible.

The first-order conditions (F.O.C.'s) are:

$$\frac{\partial \mathcal{L}}{\partial q_x} = 0 \Longrightarrow u'(q_x + q_y) = c_v + r(\underline{c}_x + \zeta\lambda_B) + \eta - \gamma_x \tag{3.5}$$

$$\frac{\partial \mathcal{L}}{\partial q_y} = 0 \Longrightarrow u'(q_x + q_y) = c'_y(q_y) - \gamma_y \tag{3.6}$$

$$\frac{\partial \mathcal{L}}{\partial k} = 0 \Longrightarrow \lambda_K = c'_k(k) - \gamma_k \tag{3.7}$$

$$\frac{\partial \mathcal{L}}{\partial \delta} = 0 \Longrightarrow \lambda_K K = \gamma_\delta \tag{3.8}$$

together with the usual complementary slackness conditions.

The co-state variables satisfy the following conditions when time differentiable:

$$\dot{\lambda}_B = \rho\lambda_B - \frac{\partial \mathcal{L}}{\partial B} \Longrightarrow \dot{\lambda}_B = \rho\lambda_B - \nu_B, \quad \nu_B \geq 0, \quad \nu_B B = 0 \tag{3.9}$$

$$\dot{\lambda}_K = \rho\lambda_K - \frac{\partial \mathcal{L}}{\partial K} \Longrightarrow \dot{\lambda}_K = (\rho + \delta)\lambda_K + m - \eta - \nu_K, \quad \nu_K \geq 0, \quad \nu_K K = 0 \tag{3.10}$$

The transversality condition at infinity reads:

$$\lim_{t\to\infty} e^{-\rho t}[\lambda_B(t)B(t) + \lambda_K(t)K(t)] = 0 \ . \tag{3.11}$$

3.2 Some properties of the optimal plans

Carbon rent

Under the constant average extraction cost assumption A.4 and the C.U.E industry competitiveness assumption A.6, the initial carbon budget B_0 must be exhausted in finite time.[8] Then equation (3.9) with $\nu_B = 0$ implies that the shadow cost of carbon pollution follows the standard Hotelling rule under a binding carbon constraint:

$$\lambda_B(t) = \lambda_{B_0} e^{\rho t}, \quad \lambda_{B_0} = \lambda_B(0), \quad t \leq t_B \ , \tag{3.12}$$

where t_B is the date of carbon budget exhaustion.

Here, $\lambda_B(t)$ is the social cost of carbon, expressed in dollars per $GtCO_2$, while $\zeta\lambda_B(t)$ is the optimal carbon tax expressed in dollars per unit of fossil fuel input (e.g., per barrel of oil).

Gross and net margins of the C.U.E industry and shadow value of the C.U.E production capacity

[8] See Appendix A for a proof in the present context. The proof uses properties of the optimal paths proven in Section **??**.

The multiplier η is the shadow marginal current value of the C.U.E production capacity. At any time t at which the C.U.E industry is active, $q_x(t) > 0$ and $\gamma_x(t) = 0$, so that from (3.5):

$$q_x(t) > 0 \Longrightarrow \eta(t) = u'(q(t)) - [c_v + r(\underline{c}_x + \zeta\lambda_B(t))] \ . \tag{3.13}$$

Since $u'(q(t)) = p(t)$, the marginal surplus, $\eta(t)$ appears as the current gross margin of the C.U.E industry when the price of the fossil fuel input is equal to its full marginal cost, which includes the resource cost $\underline{c}_x$ and the carbon tax $\zeta\lambda_B(t)$.

Subtracting the unitary maintenance cost of capital from the gross margin yields the net operational margin, $\beta(t) \equiv \eta(t) - m$. Then, for any time period during which the C.U.E industry does not scrap production capacity ($\delta(t) = 0$), equation (3.10) may be rewritten as:

$$\dot{\lambda}_K(t) = \rho\lambda_K(t) - \beta(t) \ , \tag{3.14}$$

where $\rho\lambda_K$ is the rental price of a piece of equipment valued at λ_K. Equation (3.14) states that the shadow marginal value of the installed capacity increases or decreases depending on whether its rental cost exceeds or falls below the net margin.

C.U.E production capital ends its active life when the carbon budget is exhausted. Hence at the time t_B, $\lambda_K(t_B) = 0$, since the dedicated capital becomes useless in the absence of fossil fuel use. However, as shown in Section 4, C.U.E production capacity begins to be scrapped before the budget is fully exhausted. During the scrapping phase ($\delta(t) > 0$), $\gamma_\delta = 0$, and since $K(t) > 0$ (scrapping requires existing equipment), condition (3.8) is satisfied if and only if:

$$\lambda_K(t) = 0.$$

Thus, denoting by t_δ the time at which the scrapping phase begins and integrating (3.14) over the interval $[t, t_\delta]$, for $0 \leq t \leq t_\delta$, yields:

$$\lambda_K(t) = \int_t^{t_\delta} \beta(\tau) e^{-\rho(\tau - t)} d\tau \ . \tag{3.15}$$

This means that the shadow marginal value of installed capital equals the sum of the discounted future net margins of the C.U.E industry up to the point when scrapping begins.

Full marginal cost of C.U.E and marginal cost of capital

In (3.5), the full cost of C.U.E appears as the sum of monetary costs $c_v + r\underline{c}_x$ in both the C.U.E and fossil fuel supply chain, the shadow marginal cost of carbon emissions, $\zeta r\lambda_B$,

and the multiplier associated with the capacity constraint, η. The alternative expression of η given by (3.10) allows to interpret η as the shadow marginal cost of capital use.

Using (3.10) for time periods during which the capital is not scrapped ($\delta(t) = 0$), we obtain:

$$\eta = \rho\lambda_K - \dot{\lambda}_K + m.$$

Substituting this into (3.5) results in:

$$u'(q_x + q_y) = c_v + r(\underline{c}_x + \zeta\lambda_B) + m + \rho\lambda_K - \dot{\lambda}_K \ ,$$

where the term $m + \rho\lambda_K - \dot{\lambda}_K$ is the full marginal cost of capital use. Using capital requires incurring a maintenance cost m. To this must be added its rental cost $\rho\lambda_K$, from which must be subtracted its capital gain or loss $\dot{\lambda}_K$. This is a local arbitrage condition under the assumption that the price of equipment is λ_K and the social rate of discount is ρ.

Assuming that the maintenance cost m is borne by the user, suppose that the rental payment at time $t + dt$ over the interval $[t, t + dt]$ is some amount $g(t + dt)$ less than $[\rho\lambda_K - \dot{\lambda}_K]dt$. Then the owner would prefer to sell the equipment at time t for price $\lambda_K(t)$ and earn return $\rho\lambda_K dt$. Under the rental option, the owner's asset value at $t + dt$ becomes $\lambda_K + \dot{\lambda}_K dt + g(t + dt)$, whereas under the sale option it becomes $(1 + \rho)\lambda_K(t)$. If $g(t + dt) < (\rho\lambda_K - \dot{\lambda}_K)dt$, the owner would demand a sale price higher than $\lambda_K(t)$.

We will show in the next section that $\dot{\lambda}_K(t)$ is initially negative up to the point when the C.U.E industry begins to decline. Thus, the full marginal cost of capital use is initially greater than $m + \rho\lambda_K(t)$. At this stage, capital is relatively scarce, given the size of the remaining carbon budget and the amount of fossil-based U.E still to be produced. However, over time, this scarcity decreases. Once the carbon budget becomes sufficiently tight, capital is no longer a binding constraint, its shadow value λ_K drops to zero, and the marginal cost of using capital reduces to the maintenance cost m.

Benchmarks and useful auxiliary functions

The following functions summarize some necessary relations between the C.U.E industry capacity, K, the production of S.U.E, q_y, the total production, q, and the sum of the shadow value components of the C.U.E industry marginal cost, which we denote by μ:

$$\mu \equiv \zeta r\lambda_B + \eta.$$

These functions will be repeatedly used to characterize the optimal paths.

First note that there exists a critical level of C.U.E production capacity below which

the S.U.E industry is active and above which it is no longer competitive. Let us denote this critical level by K_y, defined as the solution of $u'(K) = \underline{c}'_y$, hence $K_y > \tilde{q}_y$.

Let us denote by $\hat{q}_y(K)$ and $\hat{q}(K)$ respectively the optimal production of the S.U.E industry and the total U.E production as functions of the C.U.E production $q_x = K$: $\hat{q}(K) = K + \hat{q}_y(K)$. From the definition of K_y and the F.O.C. (3.6) with respect to q_y, we get:

$$\hat{q}_y(K) : \begin{cases} = \tilde{q}_y, & K = 0 \\ \in (0, \tilde{q}_y), & 0 < K < K_y \\ = 0, & K_y \leq K \end{cases}, \quad \frac{d\hat{q}_y}{dK} = \begin{cases} \frac{u''}{c''_y - u''} \in (-1, 0), & 0 < K < K_y \\ 0, & K_y \leq K \end{cases}. \tag{3.16}$$

$$\hat{q}(K) : \begin{cases} = \tilde{q}_y, & K = 0 \\ \in (\tilde{q}_y, K_y), & 0 < K < K_y \\ = K, & K_y \leq K \end{cases}, \quad \frac{d\hat{q}}{dK} = \begin{cases} \frac{c''_y}{c''_y - u''} \in (0, 1), & 0 < K < K_y \\ 1, & K_y \leq K \end{cases}. \tag{3.17}$$

Now consider the critical level of K denoted by K_μ for which the F.O.C. (3.5) with respect to q_x is satisfied when $\mu = 0$ and $q_y = \hat{q}_y(K)$ is optimal. Then K_μ solves:

$$u'(K + \hat{q}_y(K)) = c_v + r\underline{c}_x.$$

Since μ must be non-negative, the function $\hat{\mu}(K)$ — the value of μ satisfying the F.O.C. — is decreasing on $[0, K_\mu)$:

i) If $c_v + r\underline{c}_x > \underline{c}'_y$, then $K_\mu < K_y$ and

$$\hat{\mu}(K) > 0, \quad 0 \leq K < K_\mu, \quad \text{and} \quad \frac{d\hat{\mu}}{dK} = \frac{u''c''_y}{c''_y - u''} < 0\,. \tag{3.18}$$

ii) If $\underline{c}'_y > c_v + r\underline{c}_x$, then $K_y < K_\mu$ and

$$\hat{\mu}(K) > 0, \quad 0 \leq K < K_\mu, \quad \text{and} \quad \frac{d\hat{\mu}}{dK} = \begin{cases} \frac{u''c''_y}{c''_y - u''} < 0, & 0 < K < K_y \\ u'' < 0, & K_y < K < K_\mu \end{cases}. \tag{3.19}$$

Note that $\hat{q}_y(K)$, $\hat{q}(K)$, and $\hat{\mu}(K)$ (if $K_y < K_\mu$) are not differentiable at K_y (see Appendix A):

$$\left.\frac{d\hat{q}_y}{dK}\right|_{K=K_y^-} < \left.\frac{d\hat{q}_y}{dK}\right|_{K=K_y^+}, \quad \text{and} \quad \left.\frac{d\hat{q}}{dK}\right|_{K=K_y^-} < \left.\frac{d\hat{q}}{dK}\right|_{K=K_y^+} \tag{3.20}$$

$$\frac{d\hat{\mu}}{dK}\Big|_{K=K_y^-} > \frac{d\hat{\mu}}{dK}\Big|_{K=K_y^+} . \tag{3.21}$$

We now show how these functions are used to determine the qualitative properties of the optimal paths.

4 Optimal paths

All the optimal paths include four main phases: an initial phase of C.U.E production capacity building up to some maximum $\bar{K}$, followed by a phase of constant C.U.E capacity at this maximum $\bar{K}$, before entering a third phase of scrapping induced by the increasing scarcity of the carbon budget, and ending when the carbon budget is exhausted and the energy system returns to its initial renewable-only regime—the fourth and final phase. According to whether $\bar{K}$ is larger or smaller than K_y, the S.U.E sector is either temporarily closed or permanently kept active when the C.U.E sector reaches its maximum development. In the former case, the initial phase of C.U.E industry expansion includes two sub-phases: a first during which the S.U.E industry is active but declining, and a second during which the S.U.E production rate is nil. Symmetrically, the third phase—the scrapping phase—also includes two sub-phases: a first one during which the S.U.E sector remains inactive, and a second marked by the revival of S.U.E production. The sequence of phases and sub-phases, along with date notations, is summarized in Figure 1[9].

We first characterize the three phases of the active C.U.E industry, and next we determine how these phases unfold in the (K, B)-plane and examine how the paths depend on the size of the initial carbon budget B_0.

4.1 Expansion, stabilization and decline phases of the C.U.E industry

Under assumption A.6, which ensures the competitiveness of the C.U.E industry, the initial phase must involve investment in C.U.E production capital.[10] Proposition 1 shows

[9] Temporal structure of the four-phase optimal path under binding carbon constraints with $K_y < \bar{K}$. The horizontal axis measures time from initial conditions ($t = 0$) through complete fossil phase-out ($t = t_B$). Vertical markers indicate phase boundaries: $\underline{t}_y$ (solar displacement), t_k (peak capacity), t_δ (scrapping initiation), $\bar{t}_y$ (solar revival), and t_B (budget exhaustion). The expansion phase $[0, t_k)$ subdivides into periods with active solar $[0, \underline{t}_y)$ and complete displacement $[\underline{t}_y, t_k)$. The stabilization (plateau) phase $[t_k, t_\delta)$ maintains constant capacity $\bar{K}$. The Hotelling (decline) phase $[t_\delta, t_B)$ subdivides into initial decline without solar $[t_\delta, \bar{t}_y)$ and final decline with solar revival $[\bar{t}_y, t_B)$.

[10] If not, given the stationarity assumption of the model, the C.U.E industry would never develop—contradicting its assumed competitiveness.

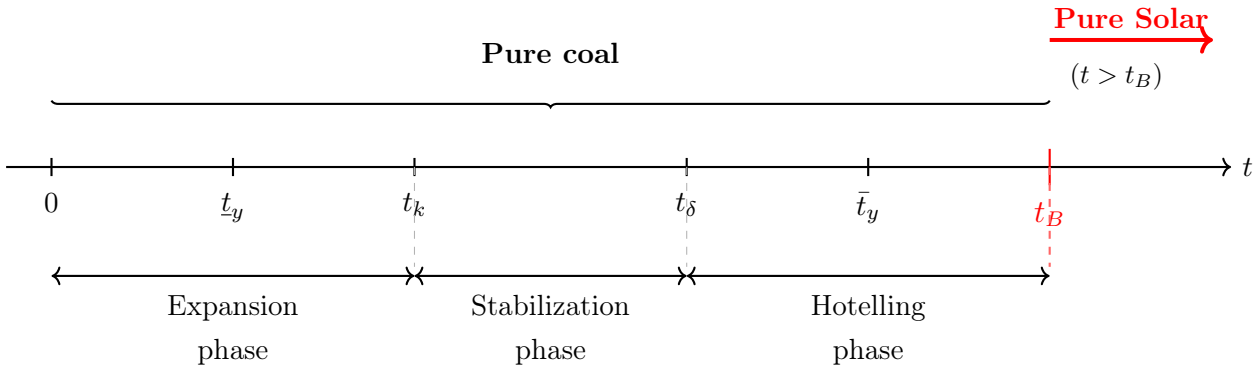

Figure 1: **Optimal Transition Timeline.** Temporal structure of the four-phase optimal path under binding carbon constraints. The "Pure coal" brace spans the fossil-based interlude from initial development ($t = 0$) until budget exhaustion ($t = t_B$). The subsequent "Pure Solar" phase represents the stationary renewable steady state attained once fossil capacity is fully phased out.

that this phase features a decreasing investment rate, and must be followed by a phase of constant capacity. Proposition 2 states that this second phase—characterized by constant C.U.E capacity—must extend until the time at which $\lambda_K(t) = 0$, provided no new round of investment occurs. Proposition 3 characterizes the decline of the C.U.E industry's production capacity during the capital scrapping phase, which is triggered by the progressive tightening of the carbon budget constraint.

Proposition P. 1 ***Expansion phase of the C.U.E industry***

Let $[0, t_k)$ be the initial time interval of investment in C.U.E production capacity: $k(t) > 0$, $t \in [0, t_k)$ and $k(t) = 0$, $t \in [t_k, t_k + \Gamma)$ for some $\Gamma > 0$. Then:

$$\dot{\lambda}_K(t) < 0, \quad t \in (0, t_k), \quad \textit{and} \quad \lim_{t \uparrow t_k} \lambda_K(t) = \underline{c}'_k. \tag{4.1}$$

Furthermore, this initial phase is followed by a phase $[t_k, t_k + \Delta)$, $\Delta > 0$, of constant industry capacity:

$$K(t) = K(t_k), \quad t \in [t_k, t_k + \Delta]. \tag{4.2}$$

Proof: Assume that $[0, t_k)$ is followed by a scrapping phase during which $\delta(t) > 0$. Then part of the capital built at $t_k - \theta$, $\theta > 0$ and small, with marginal cost at least $\underline{c}'_k > 0$, would have an infinitely short life, making cost recovery impossible.

First consider the case $K(t_k) < K_y$, so that $d\hat{\mu}/dK$ is continuous on $[0, K(t_k)]$. Assume there exists $t_1 \in (0, t_k)$ such that $\dot{\lambda}_K(t_1) \geq 0$. We show this implies $\dot{\lambda}_K(t) \geq 0$ for all $t \in (t_1, t_k)$, which leads to a contradiction.

At t_1, since $\delta(t_1) = 0$, from equation (3.14) we have:

$$\dot{\lambda}_K(t_1) = \rho\lambda_K(t_1) - \beta(t_1) \geq 0.$$

Since $\beta(t) = \eta(t) - m$, and $\eta(t) = \mu(t) - \zeta r\lambda_B(t)$, then:

$$\dot{\eta}(t) = \dot{\mu}(t) - \zeta r\dot{\lambda}_B(t) = \dot{\mu}(t) - \zeta r\rho\lambda_B(t),$$

using the Hotelling rule for the carbon shadow price. Now, since $\dot{K}(t_1) = k(t_1) > 0$, and from (3.18) $d\hat{\mu}/dK < 0$, we have $\dot{\mu}(t_1) < 0$, implying $\dot{\eta}(t_1) < 0$ and hence $\dot{\beta}(t_1) < 0$.

Therefore, for small $dt > 0$:

$$\lambda_K(t_1 + dt) \geq \lambda_K(t_1), \quad \beta(t_1 + dt) \leq \beta(t_1),$$

implying:

$$\dot{\lambda}_K(t_1 + dt) = \rho\lambda_K(t_1 + dt) - \beta(t_1 + dt) \geq 0.$$

By repetition, $\dot{\lambda}_K(t) \geq 0$ for all $t \in (t_1, t_k)$, and since $k(t_1) > 0$, from (3.7), $\lambda_K(t_1) = c_k'(k(t_1)) > \underline{c}_k'$, hence:

$$\lim_{t \uparrow t_k} \lambda_K(t) > \underline{c}_k'.$$

But since $k(t) = 0$ for $t \in (t_k, t_k + \Delta)$, then by (3.7) $\lambda_K(t) \leq \underline{c}_k'$ on this interval. A discontinuous jump down in λ_K at t_k would contradict its continuity (Seierstad and Sydsaeter, 1987, Theorem 16, p. 244).

Now consider the case $K(t_k) > K_y$ and let $\underline{t}_y$ be the time such that $K(\underline{t}_y) = K_y$. At $K = K_y$, $d\hat{\mu}/dK$ has a downward jump (see 3.21). If $t_1 \in (\underline{t}_y, t_k)$, the same argument applies since $d\hat{\mu}/dK$ is continuous over $(K_y, K(t_k))$.

If $t_1 \in (0, \underline{t}_y)$, apply the argument on $(t_1, \underline{t}_y)$, yielding $\lambda_K(\underline{t}_y^-) \geq \lambda_K(t_1)$ and $\beta(\underline{t}_y^-) \leq \beta(t_1)$. Continuity of λ_K and β implies $\dot{\lambda}_K(\underline{t}_y)$ is well-defined and ≥ 0, allowing the argument to continue over $(\underline{t}_y, t_k)$ and again yield:

$$\lim_{t \uparrow t_k} \lambda_K(t) > \underline{c}_k',$$

which contradicts the necessary continuity at t_k.[11] ■

Corollary 1 *During the initial phase $[0, t_k)$ of investment in C.U.E production capacity, the speed of capital accumulation decreases from a positive value at the start to zero at the end of the phase.*

Proposition P. 2 ***Phase of maximal expansion and stabilization of the C.U.E industry***

[11] The jump in $d\hat{\mu}/dK$ at $K = K_y$ implies a jump in $\ddot{\lambda}_K(t)$, not in $\dot{\lambda}_K(t)$.

There exists an extension $[t_k, t_\delta)$ *of the time interval* $[t_k, t_k + \Delta)$ *during which* $K(t) = K(t_k)$*, such that the net operation margin* $\beta(t)$ *decreases over this interval down to zero at time* t_δ*. Provided that* $\beta(t) = 0$ *for* $t \in (t_\delta, t_B)$*, the shadow value of capital* $\lambda_K(t)$ *decreases over this interval down to zero at time* t_δ*.*

Proof: During this phase, $q(t) = \hat{q}(K(t_k))$ is constant and

$$\beta(t) = \eta(t) - m = u'(q(t)) - [c_v + r(\underline{c}_x + \zeta\lambda_B(t)) + m]\,.$$

Since $\lambda_B(t)$ increases with t due to the Hotelling rule $\dot{\lambda}_B = \rho\lambda_B$, we have $\dot{\beta}(t) < 0$, so there exists t_δ such that $\beta(t_\delta) = 0$.

Assuming $\beta(t) = 0$ for $t \in (t_\delta, t_B)$ and using equation (3.15), since $\lambda_K(t_\delta) = 0$, we get:

$$\begin{aligned}\lambda_K(t) &= \int_t^{t_\delta} \beta(\tau) e^{-\rho(\tau - t)} d\tau \\ &< \beta(t) \int_t^{t_\delta} e^{-\rho(\tau - t)} d\tau \\ &= \frac{\beta(t)(1 - e^{-\rho(t_\delta - t)})}{\rho} \equiv h(t) > 0.\end{aligned}$$

Now from equation (3.14):

$$\frac{\dot{\lambda}_K(t)}{\lambda_K(t)} = \rho - \frac{\beta(t)}{\lambda_K(t)} < \rho - \frac{\beta(t)}{h(t)} = -\frac{\rho e^{-\rho(t_\delta - t)}}{1 - e^{-\rho(t_\delta - t)}} < 0. \tag{4.3}$$

Thus, $\dot{\lambda}_K(t) < 0$. ■

Proposition P. 3 ***Hotelling phase of capital scrapping***

If $\beta(t) = 0$ *for* $t \in (t_\delta, t_B)$*, then:*

a. The final phase of C.U.E production follows the Hotelling path under a carbon budget constraint. The marginal cost of U.E is equal to its full marginal cost, $p(t) = c_v + r(\underline{c}_x + \zeta\lambda_B(t)) + m$*, with* $p(t_B) = \tilde{p}$*.*

b. This phase is characterized by scrapping of the C.U.E capital stock. Capacity $K(t)$ *decreases from* $K(t_k)$ *at time* t_δ *down to zero at* t_B*, with* $\dot{K}(t) = \dot{q}_x(t)$*. Simultaneously, the carbon budget* $B(t)$ *decreases from* $B(t_\delta)$ *to zero at* t_B*, with* $\dot{B}(t) = -\zeta r q_x(t)$*.*

Proof: If $\beta(t) = 0$, then $\eta(t) = m$, and the F.O.C. (3.5) reduces to:

$$u'(q(t)) \equiv p(t) = c_v + r(\underline{c}_x + \zeta\lambda_B(t)) + m.$$

Differentiating with respect to time gives:

$$\dot{q}(t) = \frac{\zeta r \rho \lambda_B(t)}{u''(q(t))} < 0, \quad t \in (t_\delta, t_B).$$

From $K(t) = q_x(t) = q(t) - \hat{q}_y(K(t))$, and using equation (3.17), we get:

$$\dot{q}_x(t) = \dot{K}(t) = \begin{cases} \dot{q}(t) < 0, & K(t) > K_y \\ \dfrac{\dot{q}(t)}{1 + d\hat{q}_y/dK} < 0, & K(t) < K_y \end{cases}, \quad \delta(t) = -\frac{\dot{q}_x(t)}{q_x(t)} > 0 \tag{4.4}$$

$$\dot{q}_y(t) = \begin{cases} 0, & K(t) > K_y \\ \dfrac{d\hat{q}_y}{dK}\dot{K}(t), & K(t) < K_y \end{cases} \tag{4.5}$$

Let $\bar{t}_y$ be the time at which $K(t) = K_y$, if $\bar{K} > K_y$. Then:

$$\dot{q}_x(\bar{t}_y^-) = \dot{K}(\bar{t}_y^-) > \dot{K}(\bar{t}_y^+) = \dot{q}_x(\bar{t}_y^+), \quad \delta(\bar{t}_y^-) < \delta(\bar{t}_y^+), \quad \dot{q}_y(\bar{t}_y^-) = 0 < \dot{q}_y(\bar{t}_y^+). \tag{4.6}$$

■

4.2 The phase diagram in the (K, B) plane

Our objective is to characterize the optimal evolution trajectories of the coal and solar energy industries for a range of possible levels of the carbon budget. We want to identify the critical configuration of the carbon budget and the coal energy conversion capital such that the industry should start immediately to scrap its capacities when having to comply with the carbon budget. We want also to assess the carbon budget-coal energy production capital combination for which the industry should not try to expand its capacity and just maintain it for some time, before having to scrap its capacities when the remaining carbon budget becomes tight. We adopt a geometric approach picturing these critical configurations by means of a phase diagram in the carbon budget-coal energy capital plane. The critical configurations are described by two frontiers in this plane, we call respectively the *Stabilization-Scrapping* frontier and the *Expansion-Stabilization* frontier. To build the diagram we proceed backwards, first characterizing the Stabilization–Scrapping frontier, and then the Expansion–Stabilization one.

4.2.1 The Stabilization–Scrapping or Hotelling frontier

Let K_δ and B_δ be, respectively, the C.U.E production capacity and the remaining carbon budget at the beginning of the Hotelling phase. We denote by $K_H(B_\delta)$ the frontier function: $K_H(B_\delta)$ is the C.U.E capacity required to follow the Hotelling path starting at t_δ with a carbon budget B_δ.

Because $q_x(t)$ is decreasing during the Hotelling phase, maintaining a capacity greater than current production would be unnecessarily costly. Hence $K(t) = q_x(t)$ for $t \in (t_\delta, t_B)$, and $K_H(B_\delta)$ is the initial C.U.E production rate consistent with starting the Hotelling path from B_δ. If $K_\delta > K_H(B_\delta)$, then the difference must be scrapped immediately—an outcome ruled out along optimal paths.

Note that the graph of $K_H(B_\delta)$ is the Hotelling path itself: any point $(K_H(B'_\delta), B'_\delta)$ attained at some time t' corresponds to a point on a Hotelling trajectory, regardless of whether it is reached as the end of a stabilization phase or as part of an ongoing Hotelling path.

Let λ_{B_δ} be the value of the carbon shadow price λ_B at time t_δ, and $\Gamma_H(\lambda_{B_\delta})$ be the duration of the Hotelling phase. Given that at carbon budget exhaustion the U.E price must equal $\tilde{p}$, we solve:

$$c_v + r[\underline{c}_x + \zeta\lambda_{B_\delta} e^{\rho\Gamma_H}] + m = \tilde{p},$$

implying:

$$\frac{d\Gamma_H}{d\lambda_{B_\delta}} = -\frac{1}{\rho\lambda_{B_\delta}} < 0, \quad \lambda_{B_\delta} \in (0, \tilde{\lambda}_B), \quad \lim_{\lambda_{B_\delta}\downarrow 0} \Gamma_H = +\infty, \quad \lim_{\lambda_{B_\delta}\uparrow\tilde{\lambda}_B} \Gamma_H = 0, \tag{4.7}$$

where $\tilde{\lambda}_B = \frac{\tilde{p}-(c_v+r\underline{c}_x+m)}{\zeta r}$.

For $\lambda_{B_\delta} \in (0, \tilde{\lambda}_B)$ and $t \in [t_\delta, t_\delta + \Gamma_H]$, define the Hotelling price path:

$$p(t, \lambda_{B_\delta}) = c_v + r[\underline{c}_x + \zeta\lambda_{B_\delta} e^{\rho(t-t_\delta)}] + m.$$

Let $q(t, \lambda_{B_\delta})$, $q_x(t, \lambda_{B_\delta})$ and $q_y(t, \lambda_{B_\delta})$ be the corresponding U.E, C.U.E, and S.U.E production rates. Since $K(t) = q_x(t, \lambda_{B_\delta})$, the F.O.C. (3.5) becomes:

$$\begin{aligned} u'(q(t, \lambda_{B_\delta})) &= u'(q_x(t, \lambda_{B_\delta}) + q_y(t, \lambda_{B_\delta})) \\ &= u'(q_x(t, \lambda_{B_\delta}) + \hat{q}_y(q_x(t, \lambda_{B_\delta}))) \\ &= c_v + r[\underline{c}_x + \zeta\lambda_{B_\delta} e^{\rho(t-t_\delta)}] + m. \end{aligned}$$

Differentiating with respect to λ_{B_δ} and using the chain rule:

$$\frac{\partial q(t, \lambda_{B_\delta})}{\partial \lambda_{B_\delta}} = \frac{1}{\rho\lambda_{B_\delta}} \frac{\partial q}{\partial t}, \quad t \in (t_\delta, t_\delta + \Gamma_H). \tag{4.8}$$

From this and (4.4), (4.5) we get:

$$\frac{\partial q_x(t, \lambda_{B_\delta})}{\partial \lambda_{B_\delta}} = \frac{1}{\rho\lambda_{B_\delta}} \frac{\partial q_x}{\partial t} < 0, \quad t \in (t_\delta, t_\delta + \Gamma_H), \quad t \neq \bar{t}_y \text{ if } q_x(t_\delta) > K_y; \tag{4.9}$$

$$\frac{\partial q_x(\bar{t}_y^-, \lambda_{B_\delta})}{\partial \lambda_{B_\delta}} > \frac{\partial q_x(\bar{t}_y^+, \lambda_{B_\delta})}{\partial \lambda_{B_\delta}}, \quad \text{if } q_x(t_\delta) > K_y. \tag{4.10}$$

And for q_y:

$$\frac{\partial q_y}{\partial \lambda_{B_\delta}} = \frac{1}{\rho \lambda_{B_\delta}} \frac{\partial q_y}{\partial t} = \begin{cases} 0, & t \in (t_\delta, \bar{t}_y), \quad \text{if } q_x(t_\delta) > K_y, \\ > 0, & t \in (\bar{t}_y, t_\delta + \Gamma_H), \quad \text{if } q_x(t_\delta) > K_y, \\ > 0, & t \in (t_\delta, t_\delta + \Gamma_H), \quad \text{if } q_x(t_\delta) < K_y. \end{cases} \tag{4.11}$$

Hence:

$$\frac{\partial q_y(\bar{t}_y^-, \lambda_{B_\delta})}{\partial \lambda_{B_\delta}} < \frac{\partial q_y(\bar{t}_y^+, \lambda_{B_\delta})}{\partial \lambda_{B_\delta}}, \quad \text{if } q_x(t_\delta) > K_y. \tag{4.12}$$

Determination of the optimal value of λ_{B_δ}, given B_δ, and of the slope of $K_H(B_\delta)$

The optimal value of λ_{B_δ}, given B_δ, is the one that satisfies the carbon budget exhaustion condition:

$$\zeta r \int_{t_\delta}^{t_\delta + \Gamma_H(\lambda_{B_\delta})} q_x(t, \lambda_{B_\delta}) dt = B_\delta \ . \tag{4.13}$$

Let us denote (slightly abusing notation) by $\lambda_{B_\delta}(B_\delta)$ the shadow cost of carbon at the beginning of the Hotelling phase as a function of the available carbon budget B_δ at the same date. Differentiating (4.13) and using the fact that $q_x(t_\delta + \Gamma_H(\lambda_{B_\delta}), \lambda_{B_\delta}) = 0$, we obtain:

$$\frac{d\lambda_{B_\delta}}{dB_\delta} = \frac{1}{\zeta r \int_{t_\delta}^{t_\delta + \Gamma_H(\lambda_{B_\delta})} \frac{\partial q_x(t, \lambda_{B_\delta})}{\partial \lambda_{B_\delta}} dt} < 0 \ . \tag{4.14}$$

Hence, the slope of the Hotelling frontier function is:

$$\frac{dK_H}{dB_\delta} = \frac{\partial q_x(t_\delta, \lambda_{B_\delta})}{\partial \lambda_{B_\delta}} \cdot \frac{d\lambda_{B_\delta}}{dB_\delta} > 0, \quad B_\delta \neq B_{\delta y}, \quad \text{if } K_y < \bar{K}_{\text{sup}} \ . \tag{4.15}$$

And:

$$\lim_{B_\delta \downarrow 0} K_H(B_\delta) = 0, \quad \text{and} \quad \lim_{B_\delta \uparrow \infty} K_H(B_\delta) = \bar{K}_{\text{sup}} < +\infty \ . \tag{4.16}$$

Here, $B_{\delta y}$ is the carbon budget such that $K_H(B_\delta) = K_y$ if $K_y < \bar{K}_{\text{sup}}$, and $\bar{K}_{\text{sup}}$ solves:

$$u'(K + \hat{q}_y(K)) = c_v + r\underline{c}_x + m,$$

i.e., $\bar{K}_{\text{sup}}$ is the asymptotic level of C.U.E capacity as the carbon constraint becomes non-binding (i.e., $\lambda_{B_\delta} \to 0$ or $B_\delta \to +\infty$).

Clearly, either $K_y < \bar{K}_{\text{sup}}$ or $K_y > \bar{K}_{\text{sup}}$ may occur. In the case $K_y < \bar{K}_{\text{sup}}$, the function $K_H(B_\delta)$ is not differentiable at $B_\delta = B_{\delta y}$, and from equations (4.10) and (4.15) we get:

$$\frac{dK_H(B_{\delta y}^+)}{dB_\delta} < \frac{dK_H(B_{\delta y}^-)}{dB_\delta} \ . \tag{4.17}$$

The frontier $K_H(B_\delta)$ is illustrated in Figure 2 for the case $K_y < \bar{K}_{\text{sup}}$.

Would the initial state of the system be a pair located above the frontier $K_H(B_\delta)$, such as (K', B') in Figure 2, then the optimal policy would be to scrap the excess capital $K' - K_H(B')$ at once, then move along the Hotelling frontier from $(K_H(B'), B')$ down to $(0, 0)$. However, such a state (K', B') is never attainable starting from $K(0) = 0$ for any initial carbon budget B_0.

4.2.2 The Expansion–Stabilization frontier

We proceed backward, starting from the state $(K_\delta, B_\delta, \lambda_{B_\delta})$ at the end of the stabilization phase: where $K_\delta = K_H(B_\delta)$, $\lambda_{B_\delta} = \lambda_{B_\delta}(B_\delta)$, and $K_\delta = \bar{K} = K_k \equiv K(t_k)$. Since C.U.E capacity is constant during the stabilization phase, $K(t) = \bar{K}$ for $t \in [t_k, t_\delta]$, carbon emissions are proportional to the phase duration $\Gamma_S = t_\delta - t_k$.

Let B_k be the carbon budget at the beginning of the stabilization phase. Then:

$$B_k = B_\delta + \zeta r \bar{K} \Gamma_S.$$

Let $K_S(B_k)$ denote the frontier function. Then:

$$K_H(B_\delta) = \bar{K} = K_S(B_\delta + \zeta r \bar{K} \Gamma_S).$$

We now show that the duration Γ_S is an increasing function of $\bar{K}$, so in the (K, B)-plane, the horizontal distance between $K_H(B_\delta)$ and $K_S(B_k)$ increases with $\bar{K}$, as illustrated in Figure 2, provided $\bar{K} < \bar{K}_{\max} < \bar{K}_{\text{sup}}$.

Arbitrage condition for the last installed C.U.E capital unit

For capacity to remain constant after the investment phase, the discounted sum of profit margins during the stabilization phase must equal the construction cost of the last capital unit, i.e., $\underline{c}'_k$, by Proposition 1. Hence, the arbitrage condition for optimal duration Γ_S, optimal carbon shadow price λ_{B_δ}, and capacity $\bar{K}$ reads:

$$\int_0^{\Gamma_S} \left\{ u'(\hat{q}(\bar{K})) - \left[c_v + r \left(\underline{c}_x + \zeta \lambda_{B_\delta} e^{-\rho(\Gamma_S - \tau)} \right) + m \right] \right\} e^{-\rho\tau} d\tau = \underline{c}'_k. \tag{4.18}$$

Since λ_{B_δ} is determined by the optimality condition at the transition to the Hotelling phase, where $\lambda_K = 0$, we have:

$$\zeta r \lambda_{B_\delta} = u'(\hat{q}(\bar{K})) - (c_v + r\underline{c}_x + m) \quad \Rightarrow \quad \frac{d\lambda_{B_\delta}}{d\bar{K}} < 0. \tag{4.19}$$

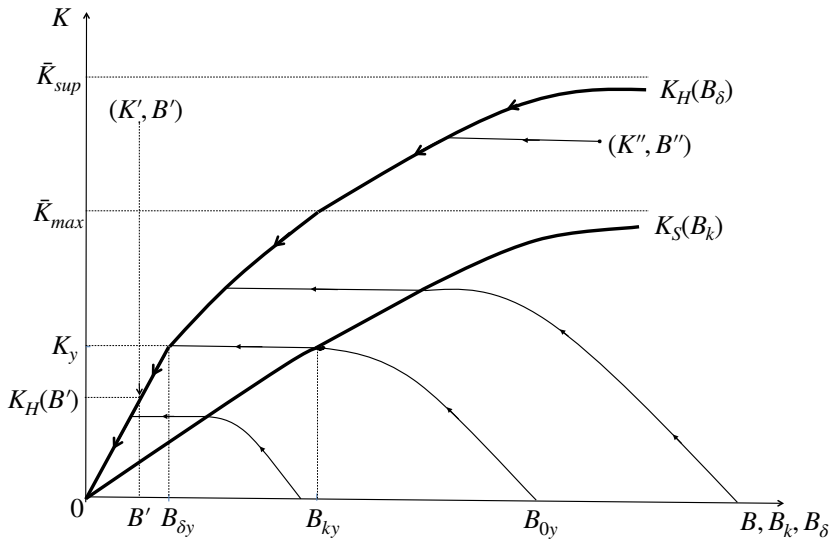

Figure 2: **Phase diagram in the** (K, B) **plane.** Optimal trajectories in the capital–carbon budget plane when $K_y < \bar{K}_{\max}$. The vertical axis is the fossil capital stock K and the horizontal axis is the remaining carbon budget B. The solid loci are thresholds: $K_S(B)$ separates expansion from the plateau, $K_H(B)$ is the Hotelling boundary where scrapping starts ($\lambda_K = 0$), and K_y is the solar-displacement threshold (horizontal line). Arrows indicate the direction of optimal motion. Starting from $(K, B) = (0, B_0)$, the economy expands: K rises while B falls. Hitting $K_S(B)$, the optimal path enters a plateau: K stays constant while B continues to decline. After crossing $K_H(B)$, scrapping begins and the system contracts, with both K and B falling until it reaches $(0, 0)$ when fossil production stops and the budget is exhausted. The diagram highlights a central implication of the model: optimal paths can feature long plateau phases with constant fossil capacity, unlike the monotone depletion paths in standard Hotelling settings.

Substituting $\lambda_{B_\delta}(\bar{K})$ into (4.18) yields:

$$\int_0^{\Gamma_S} \left\{u'(\hat{q}(\bar{K})) - (c_v + r\underline{c}_x + m)\right\} e^{-\rho\tau} d\tau - \zeta r \lambda_{B_\delta}(\bar{K}) \Gamma_S e^{-\rho\Gamma_S} = \underline{c}'_k. \tag{4.20}$$

Differentiating this with respect to $\bar{K}$, we get:

$$\begin{aligned} 0 = &\left\{u'(\hat{q}(\bar{K})) - (c_v + r\underline{c}_x + m) - \zeta r \lambda_{B_\delta}(\bar{K}) + \zeta r \rho \lambda_{B_\delta}(\bar{K}) \Gamma_S\right\} e^{-\rho\Gamma_S} d\Gamma_S \\ &+ \left\{\int_0^{\Gamma_S} \left[u''(\hat{q}(\bar{K})) \frac{d\hat{q}}{dK} - \zeta r \frac{d\lambda_{B_\delta}}{d\bar{K}} e^{-\rho\Gamma_S}\right] d\tau\right\} d\bar{K}. \end{aligned}$$

Using (4.19), we simplify the second line to:

$$u''(\hat{q}(\bar{K})) \frac{d\hat{q}}{dK} \int_0^{\Gamma_S} (e^{-\rho\tau} - e^{-\rho\Gamma_S}) d\tau \cdot d\bar{K}. \tag{4.21}$$

Therefore:

$$\frac{d\Gamma_S}{d\bar{K}} = \frac{u''(\hat{q}(\bar{K})) \frac{d\hat{q}}{dK} \int_0^{\Gamma_S} (e^{-\rho\tau} - e^{-\rho\Gamma_S}) d\tau}{-\zeta r \rho \lambda_{B_\delta}(\bar{K}) \Gamma_S e^{-\rho\Gamma_S}} > 0. \tag{4.22}$$

From:

$$\frac{d(B_k - B_\delta)}{d\bar{K}} = \zeta r \left[\bar{K} \frac{d\Gamma_S}{d\bar{K}} + \Gamma_S\right] > 0,$$

and since $\frac{dB_\delta}{d\bar{K}} > 0$ (from 4.15 with $\bar{K} = K_H$), we conclude:

$$\frac{dB_k(\bar{K})}{d\bar{K}} > 0, \quad \text{and} \quad \frac{d(B_k - B_\delta)}{d\bar{K}} > 0. \tag{4.23}$$

However, this holds only as long as there exists a pair $(\bar{K}, \Gamma_S)$ satisfying (4.20). We now show that this is true only for values $\bar{K} < \bar{K}_{\max}$, where $\bar{K}_{\max} < \bar{K}_{\sup}$, the asymptotic maximum of the Hotelling frontier. Let us assume that $e^{-\rho\Gamma_S} \lambda_{B_\delta} = \lambda_{B_k} \simeq 0$ because Γ_S is very large, so that the instantaneous net margin in the C.U.E industry is approximately:

$$u'(\hat{q}(\bar{K})) - [c_v + r\underline{c}_x + m]$$

throughout most of the stabilization phase. The capitalized value at time t_k of any equipment unit is thus no greater than:

$$\int_0^{\Gamma_S} \{u'(\hat{q}(\bar{K})) - [c_v + r\underline{c}_x + m]\} e^{-\rho\tau} d\tau.$$

At the limit when $\Gamma_S \to \infty$, the arbitrage condition (4.20) becomes:

$$u'(\hat{q}(\bar{K})) - [c_v + r\underline{c}_x + m] = \rho \underline{c}'_k. \tag{4.24}$$

Let $\bar{K}_{\max}$ denote the unique solution to (4.24). Then:

$$\bar{K}_{\max} < \bar{K}_{\sup},$$

and the arbitrage condition (4.20) can be satisfied if and only if:

$$\bar{K} < \bar{K}_{\max}.^{12}$$

To conclude:[13]

$$K_S(B_k) < \bar{K}_{\max}, \quad \frac{dK_S}{dB_k} > 0 \text{ if } B_k \neq B_{ky} \text{ and } K_y < \bar{K}_{\max}, \tag{4.25}$$

$$\lim_{B_k \downarrow 0} K_S(B_k) = 0, \quad \lim_{B_k \uparrow \infty} K_S(B_k) = \bar{K}_{\max}, \tag{4.26}$$

where B_{ky} solves $K_S(B_k) = K_y$ when $K_y < \bar{K}_{\max}$. In this case:

$$\frac{dK_S(B_{ky}^+)}{dB_k} < \frac{dK_S(B_{ky}^-)}{dB_k}. \tag{4.27}$$

If the initial state lies below the Hotelling frontier $K_H(B_\delta)$ but above the horizontal line $\bar{K}_{\max}$, as in point (K'', B'') in Figure 2, then the optimal policy is to use the available capital K'', emit $\zeta r K''$ units of carbon per unit time, until the system reaches a point on the frontier $K_H(B) = K''$. From there, it follows the Hotelling trajectory down to $(0, 0)$.

During this preliminary phase, the shadow marginal value of capital λ_K is strictly positive, starting below $\underline{c}'_k$ and decreasing to zero as the system reaches the frontier. However, such a state (K'', B'') is never encountered along an optimal trajectory beginning from $K(0) = 0$, regardless of the initial carbon budget B_0.

4.2.3 Critical carbon budget when $K_y < \bar{K}_{\max}$

If $K_y < \bar{K}_{\max}$, there exists a unique expansion path during which the C.U.E industry accumulates capital and reaches the Hotelling frontier exactly at K_y. Let B_{0y} be the initial carbon budget corresponding to this path (see Figure 2). This is the critical carbon budget below which the optimal path retains an active S.U.E industry at all

[12] Recall that $\bar{K}_{\sup}$ solves $u'(\hat{q}(\bar{K})) - (c_v + r\underline{c}_x + m) = 0$, so $\bar{K}_{\max} < \bar{K}_{\sup}$. The gap increases with $\underline{c}'_k$, i.e., $d\bar{K}_{\max}/d\underline{c}'_k < 0$.

[13] For very small B_δ, extending the duration of the stabilization phase and choosing a sufficiently small C.U.E production rate, the U.E price can be kept close to $\tilde{p} > u'(\hat{q}(\bar{K}_{\max}))$. As in the previous argument, the arbitrage condition (4.20) is satisfiable if $\tilde{p} - (c_v + r\underline{c}_x + m) \geq \rho\underline{c}'_k$, which holds strictly under Assumption A.6. Thus, a maximum feasible capacity $\bar{K}_{\max} > 0$ exists. This also implies that $\lim_{B_k \downarrow 0} \Gamma_S(B_k) > 0$.

times, and above which the S.U.E sector is temporarily shut down during the interval $(\underline{t}_y, \bar{t}_y)$ which includes the maximum capacity plateau of the C.U.E industry: $\underline{t}_y < t_k$ and $t_\delta < \bar{t}_y < t_B$.

The following proposition summarizes the structure of the optimal energy transition path.

Proposition P. 4 ***Optimal path***

Starting from a fully renewable energy system with $q(0) = q_y(0) = \tilde{q}$ and $p(0) = \tilde{p}$, the optimal transition unfolds as follows:

1. Expansion phase: During $[0, t_k)$, the capacity of the C.U.E industry increases, with $\dot{K}(t) = k(t) > 0$ and $\ddot{K}(t) = \dot{k}(t) < 0$. C.U.E production $q_x(t)$ rises, S.U.E production $q_y(t)$ declines, but total U.E production $q(t)$ increases, and the U.E price falls.

- If the S.U.E industry is highly competitive ($K_y > \bar{K}_{\max}$), it remains active regardless of the initial carbon budget B_0, though it shrinks to its minimum operational level by the end of the phase. - If the S.U.E industry is only marginally or non-competitive ($K_y < \bar{K}_{\max}$), its survival depends on B_0: - If $B_0 < B_{0y}$ (carbon-constrained), S.U.E remains active throughout. - If $B_0 > B_{0y}$ (less constrained), the C.U.E sector becomes dominant and the S.U.E industry is shut down before the plateau phase.

2. Stabilization phase: During $[t_k, t_\delta)$, the production capacities and flows of C.U.E and S.U.E are constant. This phase marks the plateau of maximum fossil-based energy output and minimal S.U.E contribution. It also corresponds to the lowest U.E price along the transition path.

3. Decline and return to renewables: During $[t_\delta, t_B)$, the final Hotelling phase unfolds: - Carbon emissions $\zeta r q_x(t)$ decline, - The carbon budget $B(t)$ is gradually depleted, - C.U.E production and capital are phased out, - The U.E price increases as fossil inputs are taxed at rising shadow cost $\zeta \lambda_B(t)$, - S.U.E production either increases or revives if it had been shut down.

However, S.U.E output cannot fully compensate for the fossil phase-down, leading to an overall decline in total U.E production. The phase concludes when $B(t_B) = 0$ — i.e., the carbon budget is exhausted — and the economy permanently reverts to its initial renewable-only regime. The fossil-based interlude ends.

The trajectories of energy quantities and prices for the case of a marginally competitive S.U.E industry and large carbon budget are illustrated in Figure 3.

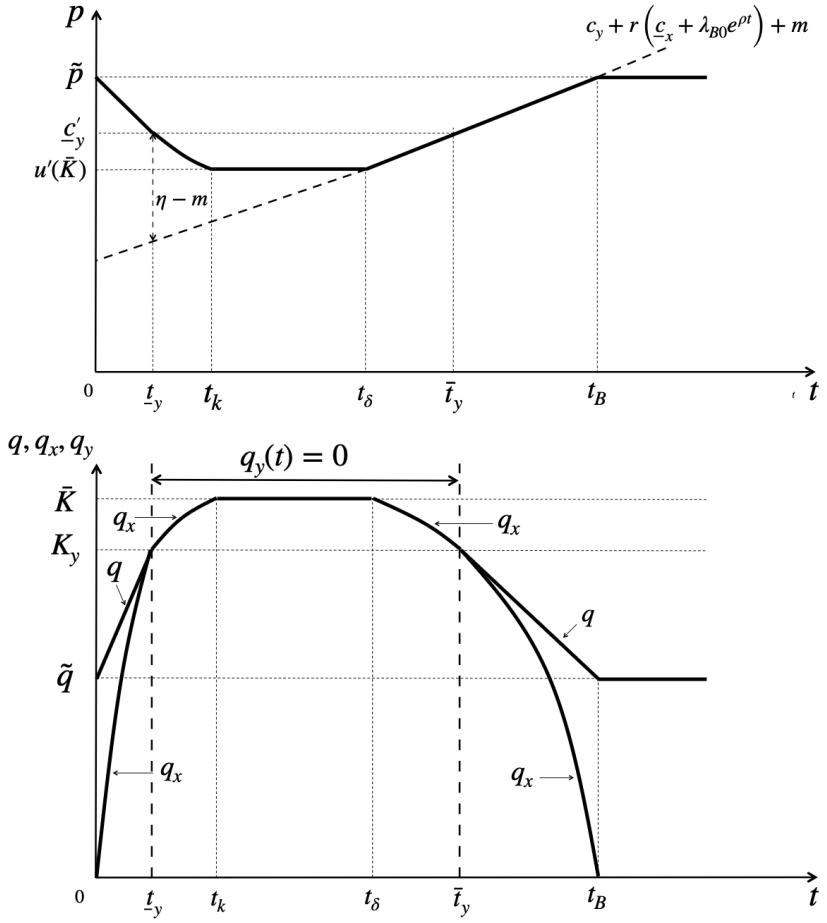

Figure 3: **Prices, quantities, and shadow values along the optimal transition.** The figure plots (i) the energy price $p(t)$ and carbon tax $\tau(t)$, (ii) energy quantities (with fossil output $q_x(t) = K(t)$ and renewable output $q_y(t)$), and (iii) the shadow value of fossil capital $\lambda_K(t)$. The energy price declines during capacity expansion, remains flat during the plateau (with $q_x(t) = \bar{K}$), and rises during phase-out; the carbon tax grows at rate ρ throughout. Renewable production is fully displaced over $[\underline{t}_y, t_\delta)$ and resumes as fossil capacity is retired, while $\lambda_K(t)$ falls to zero when scrapping begins at t_δ.

4.3 Determination of the optimal path

We now show how to use the frontier function $K_S(B_k)$ and the phase duration functions $\Gamma_S(\bar{K})$ and $\Gamma_H(\lambda_{B_\delta})$ to construct the optimal path.[14]

We first consider the cases where either $\bar{K}_{\max} < K_y$ for any B_0, or $K_y < \bar{K}_{\max}$ and $B_0 < B_{0y}$, for which the S.U.E sector remains active along the entire optimal path.

Expansion phase $[0, t_k)$:

From the F.O.C. (3.5) with $q_x(t) = K(t)$, $q_x(t) + q_y(t) = \hat{q}(K(t))$, and $\gamma_x(t) = 0$ (since $q_x(t) > 0$), we have:

$$u'(\hat{q}(K(t))) = c_v + r(\underline{c}_x + \zeta\lambda_{B_0}e^{\rho t}) + \eta(t). \tag{4.28}$$

From the co-state equation (3.10) with $\delta(t) = 0$ and $\nu_K(t) = 0$ (since $K(t) > 0$):

$$\eta(t) = -\dot{\lambda}_K(t) + \rho\lambda_K(t) + m,$$

so substituting into (4.28) yields:

$$u'(\hat{q}(K(t))) + \dot{\lambda}_K(t) - \rho\lambda_K(t) = c_v + r(\underline{c}_x + \zeta\lambda_{B_0}e^{\rho t}) + m. \tag{4.29}$$

From the F.O.C. (3.7) with $\gamma_k(t) = 0$ and $k(t) = \dot{K}(t)$, we obtain:

$$\lambda_K(t) = c_k'(\dot{K}(t)) \Rightarrow \dot{\lambda}_K(t) = c_k''(\dot{K}(t))\ddot{K}(t),$$

and substituting into (4.29):

$$u'(\hat{q}(K(t))) - \rho c_k'(\dot{K}(t)) + c_k''(\dot{K}(t))\ddot{K}(t) = c_v + r(\underline{c}_x + \zeta\lambda_{B_0}e^{\rho t}) + m. \tag{4.30}$$

For a given λ_{B_0}, denote by $K(t, \lambda_{B_0})$ a solution to (4.30) with initial condition $K(0) = 0$, and let $t_k(\lambda_{B_0})$ be the time such that $\dot{K}(t_k) = 0$, i.e., when $\lambda_K(t) = \underline{c}_k'$.

In order for $K(t, \lambda_{B_0})$, $t \in [0, t_k(\lambda_{B_0})]$, to represent the optimal expansion phase, the system's state at $t_k(\lambda_{B_0})$ must lie on the expansion–stabilization frontier. That is, the optimal value $\lambda^*_{B_0}$ solves:

$$K(t_k(\lambda_{B_0}), \lambda_{B_0}) = K_S\left[B_0 - \zeta r \int_0^{t_k(\lambda_{B_0})} K(t, \lambda_{B_0})dt\right]. \tag{4.31}$$

[14] These functions were constructed backwards from the carbon budget exhaustion point $B(t_B) = 0$, and are independent of what occurs during the initial expansion phase. Therefore, to determine the full optimal trajectory, it remains to solve for the initial expansion dynamics given $K_S(B_k)$, $\Gamma_S(\bar{K})$, and $\Gamma_H(\lambda_{B_\delta})$.

Let $\lambda^*_{B_0}$ be the unique solution. Then the optimal shadow value of capital $\lambda^*_K(t)$ during the expansion is given by:

$$\lambda^*_K(t) = c'_k(\dot{K}(t, \lambda^*_{B_0})),$$

where $\gamma_k(t) = 0$ and $k(t) = \dot{K}(t)$.

Stabilization phase $[t_k, t_\delta]$:

During this phase, the C.U.E industry capacity remains constant:

$$K(t) = \bar{K} = K(t_k(\lambda^*_{B_0}), \lambda^*_{B_0}).$$

The optimal duration $\Gamma_S(\bar{K})$ solves the arbitrage equation:

$$\int_0^{\Gamma_S} \left[u'(\hat{q}(\bar{K})) - \left(c_v + r\left(\underline{c}_x + \zeta\lambda^*_{B_0} e^{\rho[t_k(\lambda^*_{B_0})+\tau]}\right) + m\right)\right] e^{-\rho\tau} d\tau = \underline{c}'_k.$$ [15]

Over this period, the shadow value of capital $\lambda_K(t)$ declines from $\lambda_K(t_k) = \underline{c}'_k$ down to $\lambda_K(t_\delta) = 0$, where:

$$t_\delta = t_k(\lambda^*_{B_0}) + \Gamma_S(\bar{K}).$$

The carbon budget remaining at this time is:

$$B_\delta = B_0 - \zeta r \left[\int_0^{t_k(\lambda^*_{B_0})} K(t, \lambda^*_{B_0}) dt + \Gamma_S(\bar{K})\bar{K}\right].$$

Hotelling phase $[t_\delta, t_B]$:

In the final phase, C.U.E capacity is scrapped and energy production shifts back toward renewables. C.U.E production $K(t)$ satisfies:

$$u'(\hat{q}(K(t))) = c_v + r\left(\underline{c}_x + \zeta\lambda^*_{B_0} e^{\rho t}\right) + m.$$

Let $K_H(t, \lambda^*_{B_0})$ denote the solution. The phase lasts:

$$\Gamma_H(\lambda^*_{B_\delta}) = \Gamma_H(\lambda^*_{B_0} e^{\rho[t_k(\lambda^*_{B_0})+\Gamma_S(\bar{K})]}),$$

and ends at:

$$t_B = t_\delta + \Gamma_H(\lambda^*_{B_\delta}).$$

The carbon budget is exhausted exactly at this time:

$$\zeta r \left[\int_0^{t_k(\lambda^*_{B_0})} K(t, \lambda^*_{B_0}) dt + \Gamma_S(\bar{K})\bar{K} + \int_{t_\delta}^{t_B} K_H(t, \lambda^*_{B_0}) dt\right] = B_0. \tag{4.32}$$

[15] This condition equates the present value of operational margins with the marginal construction cost of C.U.E equipment.

This identity follows directly from the condition that $\lambda^*_{B_0}$ solves (4.31). Hence, the path $\{K(t), B(t)\}_{t\in[0,t_B]}$ corresponds to the optimal trajectory starting from $(0, B_0)$ in the (K, B)-plane.

In the case $\bar{K}_{\max} > K_y$ and $B_0 > B_{0y}$ (see Figure 2), the function $\hat{q}(K)$ is not differentiable at $K = K_y$ (cf. (3.17)), and the composite derivative $u'(\hat{q}(K(t)))$ changes slope at the threshold $K(t) = K_y$, occurring during both the expansion phase at time $\underline{t}_y$ and the Hotelling phase at time $\bar{t}_y$.

The technical derivations for these threshold effects are presented in Appendix A.

4.3.1 Budget exhaustion

The two–dimensional phase diagram in the (K, B)–plane provides a useful geometric summary of the optimal trajectories. Figure 2 illustrates the Hotelling frontier $K_H(B)$, the expansion–stabilization frontier $K_S(B)$, and feasible trajectories starting from $(K, B) = (0, B_0)$. Any point above the Hotelling frontier $K_H(B)$ would imply excess capital that must be scrapped immediately; such points are never reached along optimal paths starting from $K(0) = 0$. The expansion–stabilization frontier $K_S(B)$ marks the points at which the present value of operating margins during a potential plateau just equals the construction cost of marginal capital. Along the optimal path, the economy moves from $(0, B_0)$ into the region between K_S and K_H, then along K_S during the plateau, and finally along K_H as capacity is scrapped and the carbon budget is exhausted.

The proof that the carbon budget must be exhausted in finite time and that fossil exploitation must end in finite time is illustrated in Figure 4. If a positive budget remained at the end of the fossil era, the planner could profitably substitute fossil energy for renewables over a small interval, while maintaining the same total useful energy; this would violate optimality.

5 Calibration

The calibration is anchored to the global energy system around 2020. Useful energy is $q(t) = q_x(t) + q_y(t)$, where $q_x(t)$ is coal-based useful energy and $q_y(t)$ is solar-based useful energy (EJ/yr). Coal-based output requires fossil-specific conversion capacity $K(t)$ (EJ/yr). Cumulative emissions are limited by a remaining carbon budget $B(t)$ ($GtCO_2$) with $B(0) = B_0$. Welfare is discounted at the constant social rate ρ (yr^{-1}). Coal-sector parameters are mapped to coal-fired power generation, which combines high carbon intensity with long-lived dedicated capital.

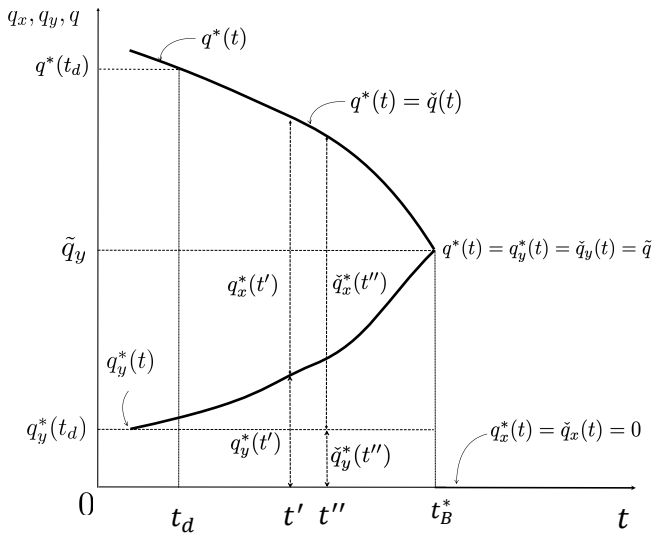

Figure 4: Optimality of complete carbon budget exhaustion. The solid curves depict a candidate optimal path that leaves unused carbon budget at t_B. The dashed curves show a locally modified path that reallocates energy production toward additional fossil use while holding total useful energy constant. Because marginal renewable costs exceed fossil marginal costs when the carbon shadow price is positive, the modified path delivers the same utility at lower cost, contradicting optimality. Therefore, any optimal path must exhaust the carbon budget exactly and terminate fossil use in finite time.

5.1 Functional forms

Instantaneous surplus from useful energy $q > 0$ is

$$u(q) = \frac{\alpha_u}{1-\sigma} q^{1-\sigma}, \qquad \sigma > 0, \tag{5.1}$$

which implies inverse demand $p(q) = u'(q) = \alpha_u q^{-\sigma}$ with constant elasticity $-1/\sigma$.

Solar supply cost is increasing and convex:

$$C_y(q_y) = c_y^{\min} q_y + \frac{\xi}{2} q_y^2, \tag{5.2}$$

where $c_y^{\min}$ (\$/GJ) is the marginal cost at the lowest-cost sites and ξ (\$/GJ^2) governs the slope of marginal cost with deployment.

Investment in fossil-specific capacity faces convex adjustment costs:

$$C_k(k) = c_k^{\min} k + \frac{\omega}{2} k^2, \tag{5.3}$$

where k is the investment flow in coal-specific capacity (GJ-cap/yr^2), $c_k^{\min}$ (\$/GJ-cap) is the marginal cost at $k = 0$, and ω governs curvature. This reduced form captures bottlenecks in specialized inputs, construction, and permitting (Sovacool et al., 2014).

Table 2: External parameters

Parameter	Symbol	Value	Unit	Source
Social discount rate	ρ	0.03	yr^{-1}	Nordhaus (2017); Drupp et al. (2018).
Carbon budget	B_0	1,150	$\mathrm{GtCO_2}$	IPCC (2021).
Carbon intensity	ζ	0.095	$\mathrm{tCO_2/GJ}$	Bituminous coal; International Energy Agency (2020a).
Fuel–capital ratio	r	2.5	—	Reciprocal of 40% efficiency; International Energy Agency (2020b).
Extraction cost	c_x	1.8	\$/GJ	Global average mine-mouth cost.
Variable O&M	c_v	4.2	\$/GJ	Non-fuel operating cost; Lazard (2021); U.S. Energy Information Administration (2021).
Fixed O&M	m	12.0	\$/GJ-cap/yr	Derived below; U.S. Energy Information Administration (2021).
Reference energy	$\tilde{q}$	580	EJ/yr	Global primary energy, 2020; International Energy Agency (2021).

5.2 External parameters

Table 2 reports parameters fixed from external sources. The baseline discount rate $\rho = 0.03$ lies between prescriptive and market-based values and is close to the median in expert surveys (Drupp et al., 2018); Section 5.7 reports sensitivity over $\rho \in [0.015, 0.05]$. The baseline carbon budget $B_0 = 1{,}150\,\mathrm{GtCO_2}$ matches the IPCC AR6 estimate for roughly 1.75°C with 50% probability from 2020 onward (IPCC, 2021, 2022). Sensitivity in B_0 addresses remaining budget uncertainty (Rogelj et al., 2019).

Fixed O&M is converted to energy-flow units as

$$m = \frac{F}{H\phi e}, \tag{5.4}$$

where F is fixed O&M (\$/kW-yr), H is annual hours, ϕ is the utilization rate, and e is the energy conversion factor (GJ/kWh). Using $F \simeq 31.5\,\$/\mathrm{kW\text{-}yr}$, $H = 8{,}760$, $\phi = 0.65$, and $e = 0.0036$ gives $m \simeq 12\,\$/\mathrm{GJ\text{-}cap/yr}$.

5.3 Internal parameters

Table 3 reports parameters chosen to match aggregate price and quantity moments around 2020.

Table 3: Internal parameters

Parameter	Symbol	Value	Unit	Calibration target
Utility curvature	σ	1.45	—	Elasticity ≈ -0.69; Labandeira et al. (2017).
Utility scale	α_u	28,140	—	$p(\tilde{q}) \simeq 28\,\$/\text{GJ}$ at $580\,\text{EJ/yr}$.
Min. capital cost	$c_k^{\min}$	20.0	\$/GJ-cap	Annualized coal plant cost; Lazard (2021).
Capital convexity	ω	0.5	—	Approx. 40% cost increase when build speed doubles; Sovacool et al. (2014).
Min. solar cost	$c_y^{\min}$	5.0	\$/GJ	Best-site PV; International Renewable Energy Agency (2021).
Solar convexity	ξ	0.012	$\$/\text{GJ}^2$	Cost–deployment gradient at $q_y \simeq 140\,\text{EJ/yr}$.

Demand. The curvature parameter $\sigma = 1.45$ implies an elasticity of -0.69, consistent with meta-analytic estimates of aggregate energy demand (Labandeira et al., 2017). The scale parameter $\alpha_u = 28{,}140$ sets $p(\tilde{q}) \approx 28\,\$/\text{GJ}$ at $\tilde{q} = 580\,\text{EJ/yr}$.

Fossil capital. The zero-investment marginal cost $c_k^{\min} = 20\,\$/\text{GJ-cap}$ is inferred from overnight coal plant costs (about \$3,700/kW), annualized over a 40-year life with a 6% capital recovery factor and mapped into capacity units using $\phi = 0.65$.[16] The curvature parameter $\omega = 0.5$ is chosen to match evidence that compressed construction schedules raise total cost materially (Sovacool et al., 2014).

Renewables. The minimum solar cost $c_y^{\min} = 5\,\$/\text{GJ}$ matches best-site utility-scale PV (International Renewable Energy Agency, 2021). The convexity parameter $\xi = 0.012\,\$/\text{GJ}^2$ matches an average solar cost of about $15.8\,\$/\text{GJ}$ at $q_y \simeq 140\,\text{EJ/yr}$ in 2020.

Lemma 1 (Interior fossil use under zero carbon pricing) *Let $\tilde{q}$ denote the renewable-only steady state defined by $u'(\tilde{q}) = C_y'(\tilde{q})$. If*

$$c_v + r c_x + m + \rho c_k^{\min} < C_y'(\tilde{q}), \tag{5.5}$$

then coal-based useful energy is used on an interior interval in the planner solution.

[16] The mapping treats K as effective annual output capacity.

Proof sketch. At $(q_x, q_y, K) = (0, \tilde{q}, 0)$, the marginal welfare gain from a small increase in coal-based output, financed by marginal investment in K, is $u'(\tilde{q})$ minus the full marginal cost in (5.5). Under the strict inequality, the deviation is locally profitable. Concavity of u and convexity of C_y and C_k then imply an interior optimum with $q_x > 0$ over some interval.

Consistency check. Without carbon pricing, the marginal cost of coal-based useful energy is

$$c_v + rc_x + m + \rho c_k^{\min} = 4.2 + 4.5 + 12.0 + 0.6 = 21.3 \text{ \$/GJ},$$

which is below $p(\tilde{q}) \approx 28$ \$/GJ and above $c_y^{\min}$. The calibration therefore supports coexistence of coal and solar at intermediate deployment levels.

5.4 Plausibility

Observed coal capacity additions during peak buildout episodes imply annual expansion rates on the order of tens of GW. Under (5.3), these rates imply marginal investment costs only moderately above $c_k^{\min}$ and therefore generate smooth accumulation rather than corner solutions. Coal generation costs of \$100–120/MWh (28–34 \$/GJ) exceed the model-implied wholesale cost because the planner problem excludes transmission, distribution, and regulatory wedges. Stranding magnitudes in the policy exercises are in the hundreds of billions of dollars when long-run targets tighten after substantial investment, which is in line with integrated-assessment estimates (Luderer et al., 2022).

5.5 Numerical method

We solve the planner's problem as a boundary-value system with states $(K(t), B(t))$ and current-value costates $(\lambda_K(t), \lambda_B(t))$, where $\lambda_B(t)$ is the shadow value of the remaining carbon budget (in \$/GtCO$_2$). For a candidate initial value $\lambda_{B0} \equiv \lambda_B(0)$, we integrate

$$\dot{K} = k - \delta K, \qquad \dot{B} = -\zeta r q_x, \tag{5.6}$$

$$\dot{\lambda}_B = \rho \lambda_B, \qquad \dot{\lambda}_K = (\rho + \delta)\lambda_K + m - \eta, \tag{5.7}$$

forward from $(K(0), B(0)) = (0, B_0)$. The multiplier $\eta(t) \geq 0$ enforces $q_x(t) \leq K(t)$. At each date, controls (q_x, q_y, k, δ) satisfy the static first-order conditions, complementary slackness, and nonnegativity.

We use an adaptive Dormand–Prince RK4/5 integrator. Regime changes are treated as events: solar inactivity ($q_y = 0$), plateau entry ($k = 0$ and $\lambda_K = c_k'(0+)$), scrapping onset ($\lambda_K = 0$), and budget exhaustion ($B = 0$). The shooting variable λ_{B0} is updated

by bracketing and bisection, with Newton refinement when smoothness permits, until implied cumulative emissions equal B_0.

Lemma 2 (Monotonicity of emissions in λ_{B0}) *Along feasible paths satisfying the static optimality conditions, cumulative emissions $\int_0^{t_B} \zeta r q_x(t)\,dt$ are weakly decreasing in λ_{B0}, with strict decrease whenever $q_x(t) > 0$ on a set of positive measure.*

Proof sketch. While $B(t) > 0$, (5.7) implies $\lambda_B(t) = \lambda_{B0} e^{\rho t}$. A higher λ_{B0} raises the effective marginal cost of coal use, $\zeta r \lambda_B(t)$, at each date. This lowers the static optimum for q_x and weakly reduces investment incentives through the shadow margin $\eta(t)$. Under feasibility and convexity, these effects cannot be offset by higher coal use at other dates, so cumulative emissions fall weakly.

Welfare along a computed path is

$$W = \int_0^{t_B} e^{-\rho t}[u(q_x + q_y) - C_y(q_y) - C_k(k) - (c_v + r c_x) q_x - mK]\,dt + \frac{e^{-\rho t_B}}{\rho}\,[u(\tilde{q}) - C_y(\tilde{q})]\,, \tag{5.8}$$

where t_B is the budget exhaustion date and the terminal term is the renewable-only continuation value.

5.6 Baseline path

Figure 5 reports the optimal transition for $B_0 = 1{,}150\,\mathrm{GtCO_2}$.

Expansion ($t \in [0, 31.5]$). Fossil capacity builds with $k(t) > 0$, and investment declines over time (about 12 EJ/yr initially and near zero by year 30). Total useful energy peaks near 600 EJ/yr, about 3% above the renewable-only level $\tilde{q}$, while the energy price falls from 28 to about 22 \$/GJ.

Plateau ($t \in [31.5, 73.8]$). Net investment stops and capacity remains at $\bar{K} \approx 215$ EJ/yr for about 42 years. The energy price stays near 22 \$/GJ. Because fossil output remains at peak capacity, the plateau accounts for 48% of cumulative emissions.

Decline ($t \in [73.8, 95.3]$). Scrapping starts when λ_K reaches zero. Capacity then falls to zero over about 21.5 years as the carbon tax rises toward \$200/tCO$_2$. The energy price rises from about 22 to 28 \$/GJ, and solar output converges to $\tilde{q}$.

Post-fossil ($t \geq 95.3$). The economy converges to the renewable-only steady state: $q = \tilde{q}$, $p = u'(\tilde{q})$, and $K = 0$.

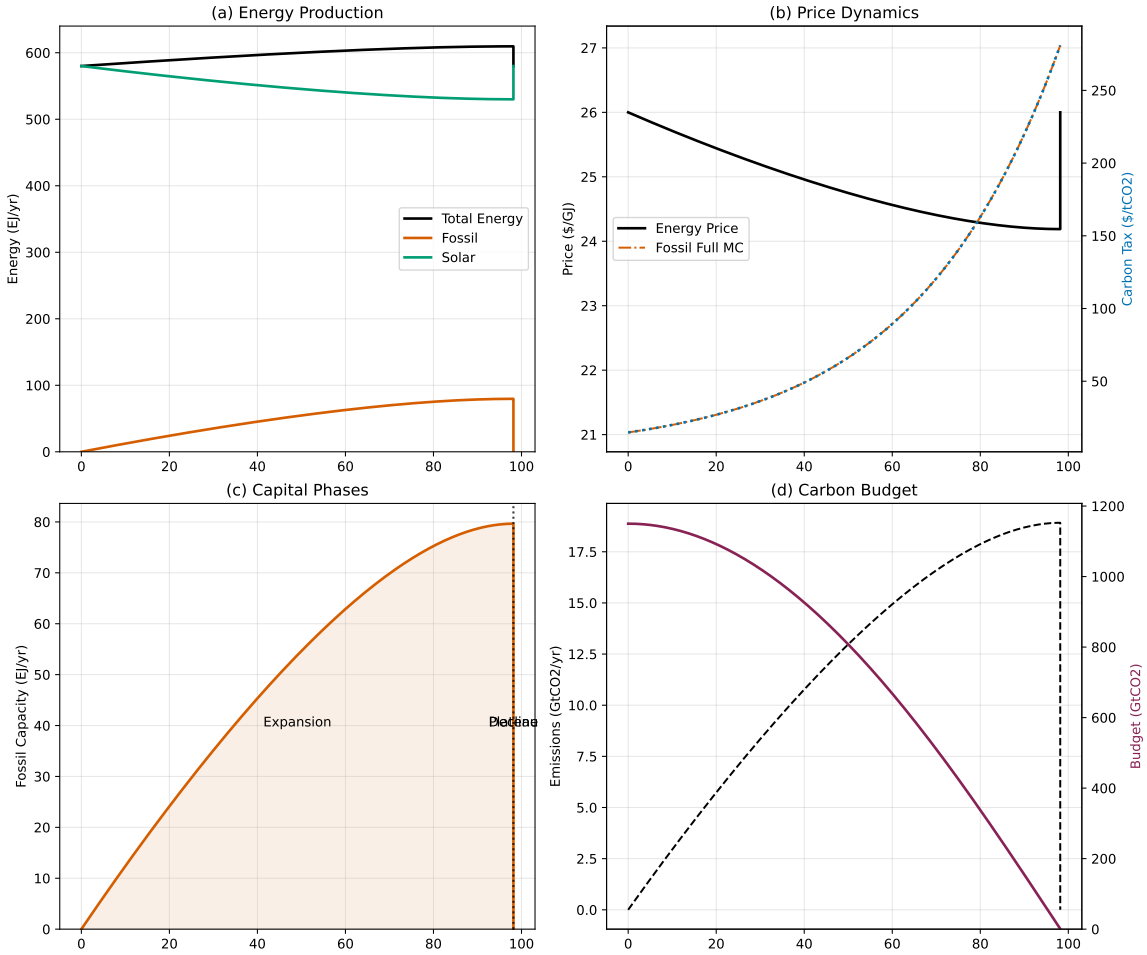

Figure 5: Baseline transition ($B_0 = 1{,}150\,\mathrm{GtCO_2}$, 1.75°C). (a) Energy quantities. (b) Energy price and carbon tax. (c) Fossil capital. (d) Cumulative emissions and remaining budget.

5.7 Sensitivity analysis

5.7.1 Carbon budget

Figure 6 reports transitions for $B_0 \in \{600, 900, 1{,}150, 1{,}400, 1{,}700\}\,\mathrm{GtCO_2}$.

Increasing B_0 from 600 to $1{,}700\,\mathrm{GtCO_2}$ extends the fossil era from about 55 to 125 years. Most of the adjustment occurs through the plateau, which lengthens from about 15 to 65 years. Expansion and decline move much less (roughly 26–35 years and 18–23 years). Peak capacity rises concavely, from about 110 to $240\,\mathrm{EJ/yr}$, so additional budget is allocated mainly through longer operation rather than proportionally higher peak buildout.

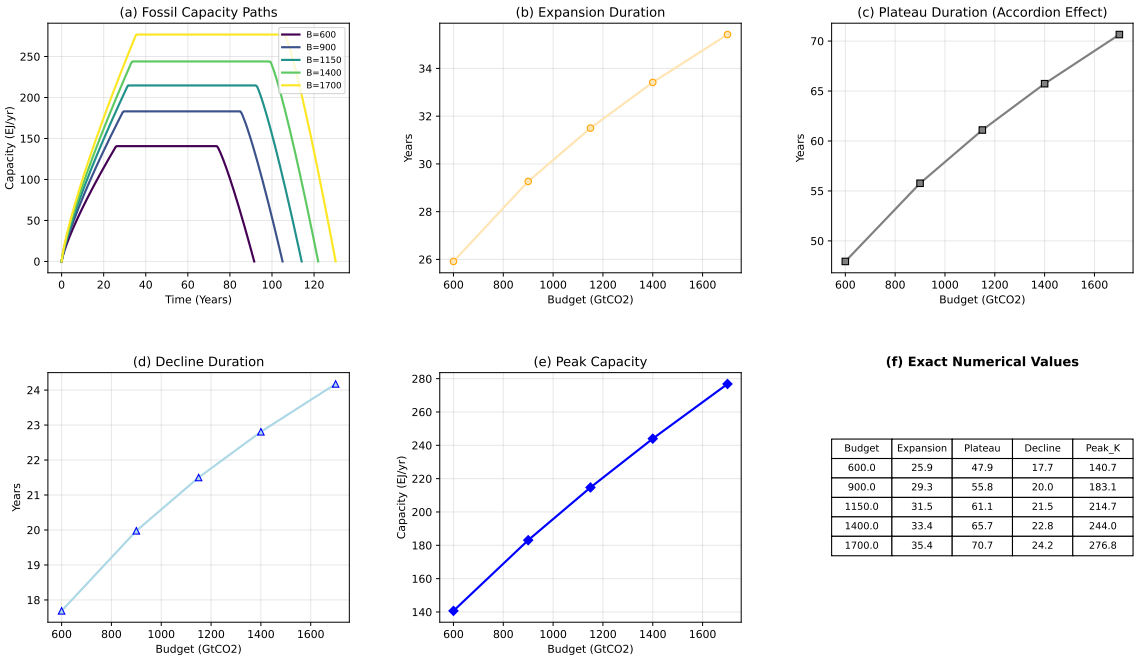

Budget	Expansion	Plateau	Decline	Peak_K
600.0	25.9	47.9	17.7	140.7
900.0	29.3	55.8	20.0	183.1
1150.0	31.5	61.1	21.5	214.7
1400.0	33.4	65.7	22.8	244.0
1700.0	35.4	70.7	24.2	276.8

Figure 6: Carbon-budget sensitivity. (a) Fossil capital paths. (b)–(d) Phase durations. (e) Peak capacity. (f) Summary values.

5.7.2 Discount rate

Figure 7 reports transitions for $\rho \in \{0.015, 0.02, 0.03, 0.04, 0.05\}$.

Lower discounting lengthens the transition and raises peak fossil capacity. As ρ falls from 5% to 1.5%, the fossil era expands from about 42 to 210 years, peak capacity rises from about 166 to 304 EJ/yr, and plateau duration rises from about 19 to 140 years. The welfare cost of the carbon constraint ranges from 0.3% ($\rho = 1.5\%$) to 5.2% ($\rho = 5\%$).

5.7.3 Renewable learning

Renewable learning is introduced through $c_y^{\min}(t) = c_y^{\min}(0)e^{-\gamma t}$ with $\gamma \in \{0, 0.04, 0.08, 0.12\}$.

At $\gamma = 0.12$, peak fossil capacity falls from 215 to 128 EJ/yr and plateau duration falls from 42 to 29 years. Solar remains active throughout the transition, including during the plateau. The effect is quantitatively comparable to large changes in B_0, consistent with complementarity between carbon pricing and innovation policy (Acemoglu et al., 2012).

5.7.4 Parameter ranking

Figure 9 reports the response of peak capacity and plateau duration to 10% increases in each parameter.

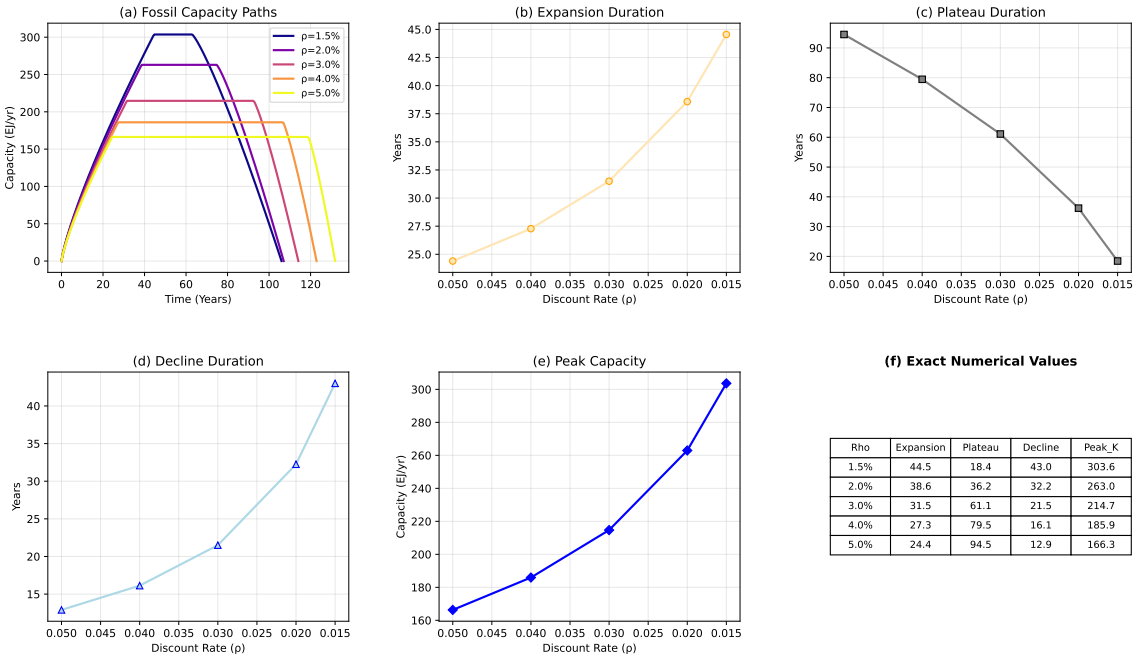

Rho	Expansion	Plateau	Decline	Peak_K
1.5%	44.5	18.4	43.0	303.6
2.0%	38.6	36.2	32.2	263.0
3.0%	31.5	61.1	21.5	214.7
4.0%	27.3	79.5	16.1	185.9
5.0%	24.4	94.5	12.9	166.3

Figure 7: Discount-rate sensitivity. (a) Fossil capital paths. (b)–(d) Phase durations. (e) Peak capacity. (f) Summary values.

Table 4: Delayed action: emissions, stranded assets, and welfare

Scenario	Emissions yrs 0–T ($GtCO_2$)	Remaining budget ($GtCO_2$)	Stranded assets ($ bn)	Post-policy duration (yrs)	Welfare loss (%)
Immediate ($T = 0$)	287	1,150	0	95	0.0
20-yr delay	486	664	287	48	1.8
40-yr delay	712	438	532	32	4.3

The carbon budget B_0 and discount rate ρ explain most of the variation. Adjustment frictions ω and learning γ are second-order in this calibration.

5.8 Policy experiments

5.8.1 Delayed action

Suppose the economy evolves without a binding carbon constraint for T years, after which the optimal carbon tax is imposed on the remaining budget. Table 4 reports outcomes for $T \in \{0, 20, 40\}$.

A 20-year delay uses 486 $GtCO_2$ and shortens the remaining transition from 95 to 48 years. Fossil capacity at policy adoption reaches 337 EJ/yr, above the level consistent

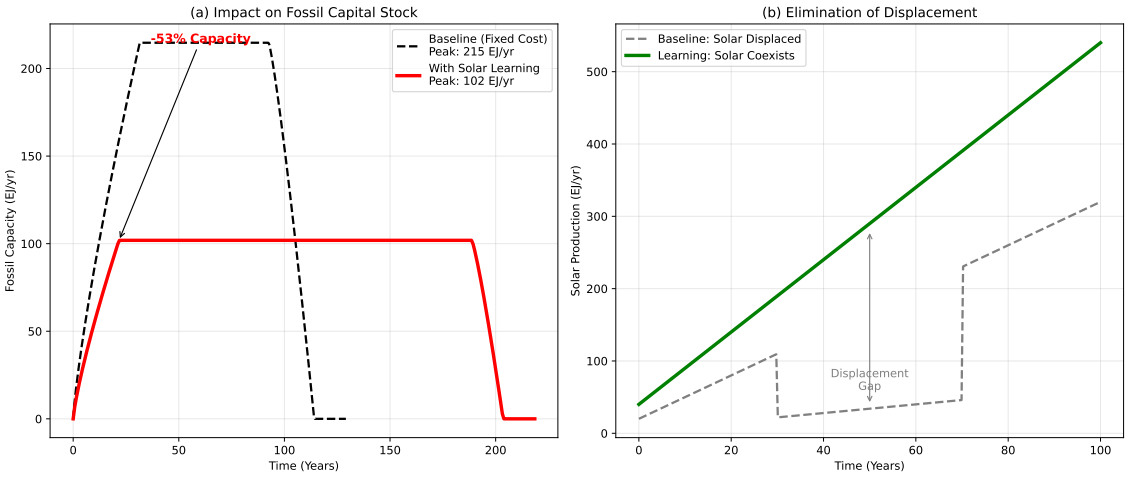

Figure 8: Renewable learning. (a) Peak fossil capacity. (b) Plateau duration. (c) Solar output paths.

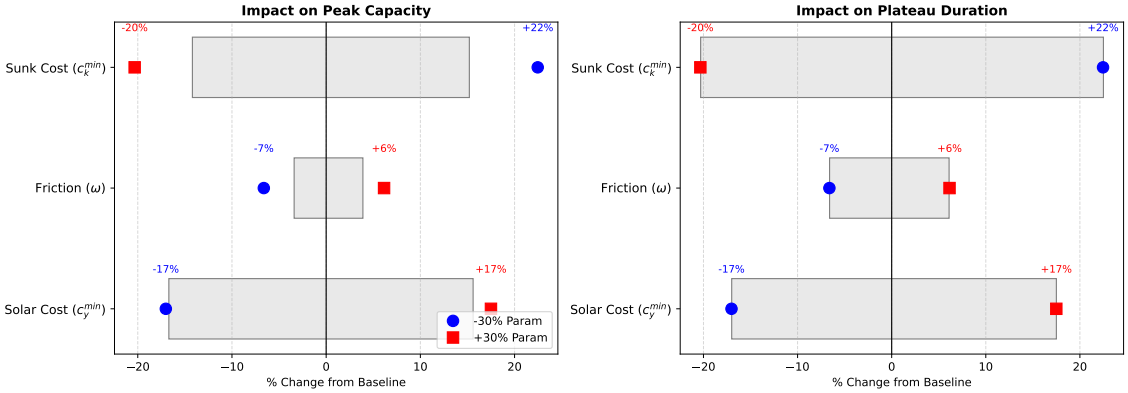

Figure 9: Parameter ranking. Percentage response of peak capacity (a) and plateau duration (b) to a 10% parameter increase.

with the remaining budget, implying \$287 bn in stranded assets. A 40-year delay raises stranding to \$532 bn and the welfare loss to 4.3%. These losses reflect premature retirement of sunk capital and compressed adjustment under a binding budget, holding climate benefits fixed (Lemoine and Traeger, 2014).

5.8.2 Unexpected tightening and stranded assets

Consider an economy planned under $B_0 = 1{,}700\,\mathrm{GtCO_2}$ and unexpectedly tightened to $1{,}150\,\mathrm{GtCO_2}$ at year 30. Under the original plan, capacity reaches $278\,\mathrm{EJ/yr}$ and cumulative emissions reach $392\,\mathrm{GtCO_2}$ by year 30. The remaining budget is then $758\,\mathrm{GtCO_2}$, consistent with capacity of only $158\,\mathrm{EJ/yr}$. The tightening therefore requires immediate scrapping of $120\,\mathrm{EJ/yr}$, valued at \$185 bn, and reduces welfare by 1.4% relative to perfect foresight under the tighter budget.

Table 5: Instrument comparison (all calibrated to the same budget)

Instrument	Peak cap. (EJ/yr)	Plateau (yrs)	Welfare loss vs. tax (%)	Notes
Carbon tax	215	42	0.0	First-best.
Capacity cap (187 EJ/yr)	187	61	0.8	Calibrated to B_0.
Investment ban (yr 25)	198	58	1.2	Calibrated to B_0.

5.8.3 Taxes versus quantity instruments

We compare three instruments, each calibrated to exhaust $B_0 = 1{,}150\,\mathrm{GtCO_2}$: (i) the first-best carbon tax $\tau(t) = \zeta r \lambda_{B0} e^{\rho t}$; (ii) a constant capacity cap $K(t) \leq \bar{K}_{\mathrm{cap}}$; and (iii) an investment ban $k(t) = 0$ for $t \geq T_{\mathrm{ban}}$.

In this homogeneous one-technology setting, calibrated quantity instruments perform close to the tax benchmark. The capacity cap shifts adjustment toward longer operation at lower peak capacity and yields a 0.8% welfare loss. The investment ban is more distortionary because it rules out capacity additions even when the shadow margin remains positive, and yields a 1.2% loss.

6 Conclusion

This paper characterizes the optimal energy transition under a cumulative carbon constraint when fossil energy requires long-lived, sector-specific capital. Capital irreversibility changes the transition problem relative to standard exhaustible-resource models and generates a distinct time profile of fossil production.

The key result is an endogenous production plateau. Over an interior region of the transition, the shadow value of fossil-specific capital declines as capacity accumulates, while the shadow value of the remaining carbon budget rises as cumulative emissions increase. When these margins offset, neither additional investment nor scrapping is optimal. Fossil capacity is therefore operated at a constant level for an extended interval, allowing sunk costs to be amortized under a binding carbon budget.

This mechanism also implies that useful-energy prices need not follow a Hotelling path. The extraction price of the fossil resource may satisfy Hotelling logic, but downstream energy prices reflect capital adjustment and carbon scarcity jointly. In the model, useful-energy prices fall during capacity expansion, remain roughly flat on the plateau, and rise during phase-out. Final energy prices are therefore not a valid proxy for testing Hotelling predictions in this environment.

Tightening the carbon budget affects transition phases asymmetrically. Expansion and decline durations move relatively little because they are governed mainly by adjustment frictions and operating conditions. Most of the adjustment occurs through the plateau, which contracts sharply as the budget tightens. In the calibration, moving from a budget consistent with 2°C to one consistent with 1.5°C primarily shortens the plateau, with smaller effects on entry and exit dates. This is the main channel through which stricter targets generate stranded assets.

The quantitative exercise is used to discipline mechanisms, not to produce forecasts. Within that scope, several implications are robust. Carbon prices rise as the budget is depleted. Sustained fossil output during the transition is not, by itself, evidence of policy failure; in the model it reflects optimal use of installed capital. Renewable learning shortens the plateau and lowers peak fossil capacity, so innovation policy and carbon pricing act through complementary margins. Delayed policy implementation or unexpected tightening increases welfare losses through premature capital retirement and compressed adjustment, even abstracting from climate damages. In the homogeneous-sector benchmark, simple quantity instruments (capacity caps) can approximate the first-best allocation with modest welfare losses relative to an optimal carbon tax.

The framework is deliberately parsimonious. The carbon budget is exogenous, renewables are represented in reduced form, scrapping is costless, and uncertainty is absent. These assumptions matter for magnitudes. They are less central for the main mechanism, which relies on the interaction between cumulative carbon scarcity and irreversible fossil capital. Extending the model to decentralized equilibrium with imperfect commitment is a natural next step for studying implementation, distribution, and political constraints.

The paper's contribution is to isolate a capital-amortization mechanism that is absent from standard transition models. Under a cumulative carbon constraint, irreversible fossil capital makes an extended plateau in fossil production an optimal feature of the transition path, not an anomaly. This result clarifies why timing, commitment, and capital specificity are central to transition policy design.

References

Acemoglu, D., Aghion, P., Bursztyn, L., and Hemous, D. (2012). The environment and directed technical change. *American Economic Review*, 102(1):131–166.

Anderson, S. T., Kellogg, R., and Salant, S. W. (2018). Hotelling under pressure. *Journal of Political Economy*, 126(3):984–1026.

Barbier, E. B. and Burgess, J. C. (2017). Depletion of the global carbon budget: A user cost approach. *Environment and Development Economics*, 22(6):658–673.

Bauer, N., Bertram, C., Luderer, G., Malik, A., and Levesque, A. (2023). Carbon budgets and the dynamics of fossil fuel markets: Pathways to rapid and orderly decarbonization. *Working Paper*.

Bauer, N., Mouratiadou, I., Luderer, G., Baumstark, L., Brecha, R., Edenhofer, O., and Kriegler, E. (2015). Global fossil energy markets and climate change mitigation: An analysis with remind. *The Energy Journal*, 36(S1):17–49.

Bommier, A., Bretschger, L., and Le Grand, F. (2018). Existence of equilibria in exhaustible markets with economics of scale and inventories. *Economic Theory*, 63(3):687–721.

Branger, F. and Quirion, P. (2014). Would border carbon adjustments prevent carbon leakage and heavy industry competitiveness losses? insights from a meta-analysis of recent economic studies. *Ecological Economics*, 99:29–39.

Cairns, R. D. (1998). The microeconomics of mineral extraction under capacity constraints. *Natural Resources Research*, 7:233–244.

Cairns, R. D. (2001). Capacity choice and the theory of the mine. *Environmental and Resource Economics*, 18(1):129–148.

Cairns, R. D. and Lasserre, P. (1986). Sectoral supply of mineral of different quality. *Scandinavian Journal of Economics*, 88(4):605–626.

Cairns, R. D. and Lasserre, P. (1991). The role of investment in multi-deposit extraction: Some results and remaining puzzles. *Journal of Environmental Economics and Management*, 21:52–66.

Campbell, H. (1980). The effect of capital intensity on the optimal rate of extraction of a mineral deposit. *Canadian Journal of Economics*, 13(2):349–356.

Coulomb, R. and Henriet, F. (2018). The grey paradox: How fossil fuel assets lock in emissions under stranded asset risk. *Journal of Environmental Economics and Management*, 87:206–223.

Crémer, J. (1979). On the hotelling's formule and the use of a permanent equipment in the extraction of natural resources. *International Economic Review*, 20(2):317–324.

Dietz, S. and Venmans, F. (2019). Cumulative carbon emissions and economic policy: In search of general principles. *Journal of Environmental Economics and Management*, 96:108–129.

Drupp, M. A., Freeman, M. C., Groom, B., and Nesje, F. (2018). Discounting disentangled. *American Economic Journal: Economic Policy*, 10(4):109–134.

Fouquet, R. (2008). *Heat, Power and Light*. Edward Elgar Publishing.

Gaudet, G. and Lasserre, P. (2022). The taxation of nonrenewable natural resources. *Annual Review of Resource Economics*, 14:415–435.

Global Energy Monitor (2023). Global coal plant tracker, january 2023 release. Technical report, Global Energy Monitor.

Global Energy Monitor (2025). Global coal plant tracker. Dataset.

Gollier, C. (2024). The cost-efficiency carbon pricing puzzle. *Journal of Environmental Economics and Management*, 128:103062.

Golosov, M., Hassler, J., Krusell, P., and Tsyvinski, A. (2014). Socially optimal climate policy. *Econometrica*, 82(1):41–88.

Hartwick, J., Kemp, M., and Long, N. V. (1986). Set-up costs and the theory of exhaustible resources. *Journal of Environmental Economics and Management*, 13:212–224.

Hassler, J. and Krusell (2018). Environmental macroeconomics: The case of climate change. *Handbook of Macroeconomics*, 4:333–394.

Hirth, L. (2015). The market value of variable renewables: The effect of solar wind power variability on their relative price. *Energy Economics*, 38:218–236.

Holland, S. (2003a). Extraction capacity and the optimal order of extraction. *Journal of Environmental Economics and Management*, 15(3):569–588.

Holland, S. (2003b). Set-up cost and the existence of competitive equilibrium when extraction capacity is limited. *Journal of Environmental Economics and Management*, 46(3):539–556.

Hotelling, H. (1931). The economics of exhaustible resources. *Journal of Political Economy*, 39:137–175.

International Energy Agency (2020a). Coal information 2020. Emission factors and energy content of coal.

International Energy Agency (2020b). Energy efficiency indicators 2020. Technical report, International Energy Agency, Paris.

International Energy Agency (2021). World energy outlook 2021. Technical report, International Energy Agency, Paris.

International Renewable Energy Agency (2021). Renewable power generation costs in 2020. Technical report, IRENA, Abu Dhabi.

IPCC (2021). *Climate Change 2021: The Physical Science Basis. Contribution of Working Group I to the Sixth Assessment Report of the Intergovernmental Panel on Climate Change*. Cambridge University Press, Cambridge, United Kingdom and New York, NY, USA.

IPCC (2022). Climate change 2022: Mitigation of climate change. contribution of working group iii to the sixth assessment report. Technical report, Intergovernmental Panel on Climate Change, Cambridge University Press.

IRENA (2023). Renewable power generation costs in 2023. https://www.irena.org.

Joskow, P. L. (2011). Comparing the costs of intermittent and dispatchable electricity generating technologies. *American Economic Review*, 101(3):238–241.

Kander, A., Malanima, P., and Warde, P. (2013). Power to the people: Energy in europe over the last five centuries. *Princeton University Press*.

Kriegler, E., Bertram, C., Kuramochi, T., Jakob, M., Pehl, M., Stevanović, M., Höhne, N., Luderer, G., Minx, J. C., Fekete, H., et al. (2023). Short term policies to keep the door open for paris climate goals. *Environmental Research Letters*, 18(7):074032.

Labandeira, X., Labeaga, J. M., and López-Otero, X. (2017). A meta-analysis on the price elasticity of energy demand. *Energy Policy*, 102:549–568.

Lasserre, P. (1982). Exhaustible resource extraction with capital. Cahier de recherche 8208, Département de Science Économique, Université de Montréal.

Lasserre, P. (1985a). Capacity choice by mines. *Canadian Journal of Economics*, 18(4):831–842.

Lasserre, P. (1985b). Exhaustible resource extraction with capital. In Scott, A. D., editor, *Progress in Natural Resource Economics*. Oxford University Press.

Lazard (2021). Levelized cost of energy analysis – version 15.0. Technical report.

Lemoine, D. and Rudik, I. (2017). Steering the climate system: Using inertia to lower the cost of policy. *American Economic Review*, 107(10):2947–2957.

Lemoine, D. and Traeger, C. (2014). Watch your step: Optimal policy in a tipping climate. *American Economic Journal: Economic Policy*, 6(1):137–166. Closely related QJE-level work.

Lozada, G. (1993). The conservationist's dilemma. *International Economic Review*, 34(3):647–662.

Luderer, G., Madeddu, S., Merfort, L., Ueckerdt, F., Pehl, M., Pietzcker, R., Rottoli, M., Schreyer, F., Bauer, N., Baumstark, L., et al. (2022). Impact of declining renewable energy costs on electrification in low-emission scenarios. *Nature Energy*, 7:32–42.

Millstein, D., Wiser, R., Mills, A. D., Bolinger, M., Seel, J., and Jeong, S. (2021). Solar and wind grid system value in the united states: The effect of transmission congestion, generation profiles, and curtailment. *Joule*, 5(2):446–471.

Nordhaus, W. D. (2017). Revisiting the social cost of carbon. *Proceedings of the National Academy of Sciences*, 114(7):1518–1523.

Olsen, T. (1989). Capital investment and resource extraction from non-identical deposits. *Journal of Environmental Economics and Management*, 17:127–139.

Pahle, M., Burtraw, D., Flachsland, C., Kelsey, N., Biber, E., Meckling, J., Edenhofer, O., and Zysman, J. (2022). Sequencing to ratchet up climate policy stringency. *Nature Climate Change*, 12:108–113.

Pfeiffer, A., Millar, R., Hepburn, C., and Beinhocker, E. (2016). The '2°C capital stock' for electricity generation: Committed cumulative carbon emissions from the electricity generation sector and the transition to a green economy. *Applied Energy*, 179:1395–1408.

Puu, T. (1977). On the profitability of exhausting natural resources. *Journal of Environmental Economics and Management*, 4:185–199.

Rennert, K., Errickson, F., Prest, B. C., Rennels, L., Newell, R. G., Pizer, W., Kingdon, C., Wingenroth, J., Cooke, R., Parthum, B., Smith, D., Cromar, K., Diaz, D., Moore, F. C., Müller, U. K., Plevin, R. J., Raftery, A. E., Ševčíková, H., Sheets, H., Stock, J. H., Tan, T., Watson, M., Wong, T. E., and Anthoff, D. (2022). Comprehensive evidence implies a higher social cost of co_2. *Nature*, 610:687–692.

Rogelj, J., Forster, P. M., Kriegler, E., Smith, C. J., and Séférian, R. (2019). Estimating and tracking the remaining carbon budget for stringent climate targets. *Nature*, 571:335–342.

Sovacool, B. K., Gilbert, A., and Nugent, D. (2014). An international comparative assessment of construction cost overruns for electricity infrastructure. *Energy Research & Social Science*, 3:152–160.

Speirs, J., McGlade, C., and Slade, R. (2015). Uncertainty in the availability of natural resources: Fossil fuels, critical metals and biomass. *Energy Policy*, 87:654–664.

Stern, D. (2011). The role of energy in economic growth. *Ecological Economics Reviews*, 1219.

Stürmer, M. (2018). 150 years of boom and bust: What drives mineral commodity prices? *Macroeconomic Dynamics*, 22(3):702–717. Related JPE-level evidence on resource price dynamics.

U.S. Energy Information Administration (2021). Capital cost and performance characteristic estimates for utility scale electric power generating technologies. Technical report, U.S. Department of Energy.

van der Ploeg, F. and Rezai, A. (2020). Stranded assets in the transition to a carbon-free economy. *Annual Review of Resource Economics*, 12(1):281–298.

Vu, T. and Im, E. (2011). Optimal fee to recover the setup cost of resource extraction. *IAENG International Journal of Applied Mathematics*, 41(2):122–127.

World Bank (2024). Carbon pricing dashboard. Data as of 2024.

Appendix

A1 Non-Differentiability at the Solar Displacement Threshold

We establish the non-differentiability of key equilibrium functions at the critical capital threshold $K = K_y$ where solar energy is completely displaced by fossil-based production. This threshold plays a central role in determining the structure of optimal transition paths under binding carbon constraints.

Consider the solar energy output function $\hat{q}_y(K)$, total useful energy $\hat{q}(K)$, and marginal surplus function $\hat{\mu}(K)$ when the carbon budget $B(t)$ depletes according to

$$\dot{B}(t) = -\zeta r q_x(t), \quad B(0) = B_0,$$

with shadow price $\lambda_B(t)$ on the remaining atmospheric capacity.

Non-differentiability of solar output $\hat{q}_y(K)$. From first-order conditions (Eq. 3.16), the left-hand derivative as K approaches K_y from below satisfies

$$\lim_{K \uparrow K_y} \frac{d\hat{q}_y}{dK} = \frac{u''(K_y)}{c_y''(0^+) - u''(K_y)}.$$

Given $u'' < 0$ (concave utility) and $c_y'' \geq 0$ (convex renewable costs), this derivative lies in $(-1, 0]$, with equality when $c_y''(0^+) = 0$ (linear renewable costs at low deployment). By contrast, for $K > K_y$ where solar production ceases,

$$\lim_{K \downarrow K_y} \frac{d\hat{q}_y}{dK} = 0.$$

This discontinuity in the marginal response reflects the discrete shift from partial to complete fossil dominance at the threshold.

Non-differentiability of total energy $\hat{q}(K)$. Total useful energy satisfies $\hat{q}(K) = K + \hat{q}_y(K)$, inheriting the kink from solar output:

$$\lim_{K \uparrow K_y} \frac{d\hat{q}}{dK} = 1 + \lim_{K \uparrow K_y} \frac{d\hat{q}_y}{dK} < 1 = \lim_{K \downarrow K_y} \frac{d\hat{q}}{dK}.$$

This non-smoothness reflects changing returns to capital accumulation as the energy mix shifts discretely.

Non-differentiability of marginal surplus $\hat{\mu}(K)$. From Eq. 3.19, the marginal surplus function exhibits

$$\lim_{K\uparrow K_y} \frac{d\hat{\mu}}{dK} = \frac{u''(K_y)\cdot c_y''(0^+)}{c_y''(0^+) - u''(K_y)} > u''(K_y) = \lim_{K\downarrow K_y} \frac{d\hat{\mu}}{dK},$$

where the inequality holds strictly when $c_y''(0^+) > 0$.

These results establish kinks at $K = K_y$ across all major equilibrium functions, driven by the discontinuous shift in optimal energy sourcing. Under carbon constraints, fossil extraction $q_x(t)$ depletes $B(t)$, creating dynamic interaction between the rising carbon shadow price $\lambda_B(t)$ and the (initially) rising, then falling capital shadow value $\lambda_K(t)$ that governs optimal transition timing.

A2 Optimal Transition Path: Phase-by-Phase Characterization

We characterize the complete optimal path by solving the necessary conditions phase by phase, tracking both state variables (K, B) and shadow prices (λ_K, λ_B) throughout the transition.

A2.1 Expansion Phase: $[0, t_k)$

A2.1.1 Early Expansion with Active Solar: $[0, \underline{t}_y)$

During initial expansion, both energy sources operate. With no scrapping ($\delta = 0$), capital accumulation follows $\dot{K} = k$ and fossil extraction equals capacity: $q_x = K$. The necessary conditions yield

$$u'\big(\hat{q}_1(K(t))\big) = c_v + r\big(c_x + \lambda_B e^{\rho t}\big) + \eta(t), \tag{AA2.1}$$

$$\eta(t) = -\dot{\lambda}_K(t) + \rho\lambda_K(t) + m, \tag{AA2.2}$$

where λ_B denotes the initial shadow price of the carbon budget and $\eta(t)$ is the shadow rent on capacity constraints.

Combining these conditions with the adjustment cost relationship $\lambda_K(t) = c_k'(\dot{K}(t))$ implies

$$c_k''(\dot{K}(t))\ddot{K}(t) = u'\big(\hat{q}_1(K(t))\big) - c_v - r\big(c_x + \lambda_B e^{\rho t}\big) - m - \rho c_k'(\dot{K}(t)).$$

This second-order differential equation in $K(t)$ governs capital dynamics, with solution denoted $K_1(t, \lambda_B)$ satisfying boundary condition $K(0) = 0$.

The sub-phase terminates at $\underline{t}_y(\lambda_B)$ when solar displacement occurs: $K_1(\underline{t}_y, \lambda_B) = K_y$. At this threshold, renewable generation becomes uncompetitive and $\hat{q}_{y1}(K_y) = 0$.

Throughout this phase, the carbon budget evolves according to

$$B(t) = B_0 - \zeta r \int_0^t K_1(s, \lambda_B)\, ds,$$

linking cumulative emissions to the investment path. This constraint shapes optimal capacity accumulation by incorporating the opportunity cost of atmospheric absorption capacity.

A2.1.2 Late Expansion without Solar: $[\underline{t}_y, t_k)$

Following solar displacement, fossil energy supplies all demand: $q = K$ and $q_y = 0$. The governing equation becomes

$$u'\big(\hat{q}_2(K(t))\big) - \rho c_k'(\dot{K}(t)) + c_k''(\dot{K}(t))\ddot{K}(t) = c_v + r\big(c_x + \lambda_B e^{\rho t}\big) + m, \tag{AA2.3}$$

with solution $K_2(t, \lambda_B)$ satisfying continuity at the switching time:

$$K_2\big(\underline{t}_y(\lambda_B), \lambda_B\big) = K_y = K_1\big(\underline{t}_y(\lambda_B), \lambda_B\big).$$

The expansion phase concludes at $t_k(\lambda_B)$ when net investment ceases: $\dot{K}_2(t_k, \lambda_B) = 0$. At this point, the capital stock reaches its peak $\bar{K} = K_2(t_k, \lambda_B)$, and the shadow value equals the minimum investment cost: $\lambda_K(t_k) = c_k'(0)$.

For the path to be optimal, terminal conditions at t_k must lie on the expansion-stabilization frontier defined by the carbon budget constraint:

$$K(t_k(\lambda_B), \lambda_B) = K_S\left(B_0 - \zeta r\left[\int_0^{\underline{t}_y(\lambda_B)} K_1(t, \lambda_B)\, dt + \int_{\underline{t}_y(\lambda_B)}^{t_k(\lambda_B)} K_2(t, \lambda_B)\, dt\right]\right). \tag{AA2.4}$$

Let λ_B^* denote the value satisfying this transversality condition. Then the complete expansion path is

$$K(t, \lambda_B^*) = \begin{cases} K_1(t, \lambda_B^*), & 0 \le t < \underline{t}_y(\lambda_B^*), \\ K_2(t, \lambda_B^*), & \underline{t}_y(\lambda_B^*) \le t < t_k(\lambda_B^*), \end{cases}$$

with corresponding shadow value

$$\lambda_K^*(t) = \begin{cases} c_k'\big(\dot{K}_1(t, \lambda_B^*)\big), & 0 \le t < \underline{t}_y(\lambda_B^*), \\ c_k'\big(\dot{K}_2(t, \lambda_B^*)\big), & \underline{t}_y(\lambda_B^*) \le t < t_k(\lambda_B^*). \end{cases}$$

A2.2 Stabilization Phase: $[t_k, t_\delta)$

Capacity remains constant throughout this phase:

$$K(t) = \bar{K} = K_2\big(t_k(\lambda_B^*), \lambda_B^*\big), \quad k(t) = \delta(t) = 0.$$

The duration $\Gamma_S(\bar{K})$ solves the arbitrage condition derived in the main text (Eq. **??**), ensuring the quasi-rent from operating existing capacity exactly covers maintenance costs plus the user cost of capital.

Setting $t_\delta = t_k(\lambda_B^*) + \Gamma_S(\bar{K})$, cumulative emissions through the plateau are

$$\int_0^{t_\delta} \zeta r q_x(t)\, dt = \zeta r \left[\Gamma_S(\bar{K}) \cdot \bar{K} + \int_0^{\underline{t}_y} K_1(t, \lambda_B^*)\, dt + \int_{\underline{t}_y}^{t_k} K_2(t, \lambda_B^*)\, dt \right],$$

leaving residual carbon budget

$$B(t_\delta) = B_0 - \zeta r \left[\Gamma_S(\bar{K})\bar{K} + \int_0^{\underline{t}_y} K_1(t)\, dt + \int_{\underline{t}_y}^{t_k} K_2(t)\, dt \right].$$

By construction, the capital shadow value falls continuously during the plateau, reaching zero at its terminus: $\lambda_K(t_\delta) = 0$. This marks the transition from capital scarcity (where investment would be profitable absent carbon constraints) to capital abundance (where scrapping becomes optimal).

A2.3 Hotelling Phase: $[t_\delta, t_B)$

A2.3.1 Initial Decline without Solar Revival: $[t_\delta, \bar{t}_y)$

Once $\lambda_K = 0$, continued operation requires that operating margins cover only maintenance costs. With solar still inactive, capacity evolves according to

$$u'\big(\hat{q}_2(K(t))\big) = c_v + r\big(c_x + \lambda_B^* e^{\rho t}\big) + m.$$

Denote the solution $K_{H2}(t, \lambda_B^*)$. This sub-phase terminates at $\bar{t}_y$ when rising carbon prices restore solar competitiveness:

$$c_v + r\big(c_x + \lambda_B^* e^{\rho \bar{t}_y}\big) + m = c_y'(0),$$

i.e., when fossil marginal cost equals the renewable backstop price.

A2.3.2 Final Decline with Solar Revival: $[\bar{t}_y, t_B)$

Both energy sources operate during the final phase, with capacity satisfying

$$u'\big(\hat{q}_1(K(t))\big) = c_v + r\big(c_x + \lambda_B^* e^{\rho t}\big) + m.$$

Fossil production ceases at t_B when operating costs exceed the long-run renewable price:

$$c_v + r\big(c_x + \lambda_B^* e^{\rho t_B}\big) + m = \tilde{p} = u'\big(\tilde{q}_y\big),$$

where $\tilde{q}_y$ denotes steady-state renewable output and $\tilde{p}$ the corresponding market-clearing price.

A3 Finite Termination and Budget Exhaustion

We establish that fossil exploitation must terminate in finite time and the carbon budget must be fully depleted at termination. The proofs proceed by contradiction. This result is illustrated in Figure 4.

A3.1 Fossil exploitation ends in finite time: $t_B < +\infty$

We consider successively the cases $\lambda_{B_0} > 0$ and $\lambda_{B_0} = 0$.

Case $\lambda_{B_0} > 0$.

Assume that there exists an infinite sequence of dates $\{t_n\}_{n=1}^{\infty}$ such that $\lim_{n\to\infty} t_n = +\infty$ and $q_x(t_n) > 0$ for all n. Then the shadow marginal operating current cost of the carbon-using energy (C.U.E.) sector at time t_n, denoted $SMOCC(t_n)$, is given by

$$SMOCC(t_n) = c_v + r(\underline{c}_x + \lambda_{B_0} e^{\rho t_n}) + m.$$

Since $\lambda_{B_0} > 0$, it follows that $\lim_{n\to\infty} SMOCC(t_n) = +\infty$. Hence there exists $\underline{n}$ such that

$$SMOCC(t_n) > \tilde{p} \quad \text{for all } n \geq \underline{n},$$

so that it would be strictly optimal to supply the renewable backstop $\tilde{q}_y$ only and set $q_x = 0$, a contradiction. □

Case $\lambda_{B_0} = 0$.

Assume first that the expansion phase ends in finite time, $t_k < \infty$. From t_k onward, the instantaneous gross margin of the C.U.E. sector equals

$$u'(\hat{q}(\bar{K})) - (c_v + r\underline{c}_x + m),$$

where $\bar{K}$ denotes installed fossil capacity at the end of expansion. The arbitrage condition determining $\bar{K}$, which must hold at t_k for the marginal unit of capacity (cf. equation (A41) with $\Gamma_S = +\infty$), is

$$\int_0^{+\infty} \{u'(\hat{q}(\bar{K})) - (c_v + r\underline{c}_x + m)\} e^{-\rho\tau} d\tau = \underline{c}'_k. \tag{AA3.5}$$

From t_k onward, fossil use equals $r\bar{K}$ at each instant, which requires an infinite carbon budget—contradicting feasibility.

Assume instead that $t_k = +\infty$, so that the expansion phase is infinite. Since $\dot{K}(t) > 0$ throughout expansion, for any $\varepsilon \in (0, \bar{K})$ there exists $\underline{t} < +\infty$ such that

$$K(t) \geq \bar{K} - \varepsilon \quad \text{for all } t \geq \underline{t},$$

where $\bar{K}$ solves (AA3.5). From $\underline{t}$ onward, fossil input is at least $r(\bar{K} - \varepsilon)$ at each instant, again requiring an infinite carbon budget. This contradiction establishes that fossil exploitation must end in finite time. □

A3.2 The carbon budget must be exhausted at time t_B

Let an asterisk denote a candidate optimal path

$$\{(q_x^*(t), q_y^*(t), k^*(t), \delta^*(t))\}_{t=0}^{\infty}$$

along which the carbon budget is not exhausted. Let

$$\underline{B} = B^*(t_B) > 0$$

denote the remaining unused budget at the terminal date. By the previous result, optimality then requires $\lambda_{B_0} > 0$.

Consider an interval (t_d, t_B^*) within the Hotelling phase, with $t_\delta^* < t_d < t_B^*$, during which $q_y^*(t) > 0$. Since renewable output is increasing once positive during this phase and

$$\lim_{t \uparrow t_B^*} q_y^*(t) = \tilde{q}_y > 0,$$

such an interval exists.

Define an alternative path

$$\{(\check{q}_x(t), \check{q}_y(t), \check{k}(t), \check{\delta}(t))\}_{t=0}^{\infty}$$

that coincides with the candidate path on $[0, t_d]$ and is modified on (t_d, t_B^*) as follows:

$$\check{q}_x(t) = \begin{cases} q^*(t) - q_y^*(t_d), & t_d < t < t_B^*, \\ 0, & t \geq t_B^*, \end{cases}$$

$$\check{q}_y(t) = \begin{cases} q_y^*(t_d), & t_d < t < t_B^*, \\ \tilde{q}_y, & t \geq t_B^*, \end{cases}$$

$$\check{\delta}(t) = \begin{cases} \dot{q}(t)/q^*(t) - q_y^*(t_d), & t_d < t < t_B^*, \\ 0, & t \geq t_B^*. \end{cases}$$

At t_B^*, the entire fossil capital stock is scrapped.

Both paths are illustrated in Figure 4.

By construction,

$$q^*(t) = q_x^*(t) + q_y^*(t) = \check{q}_x(t) + \check{q}_y(t) = \check{q}(t),$$

so utility is identical along both paths. The additional cumulative emissions required by the modified path equal

$$\Delta B(t_B^*) = \zeta r \int_{t_d}^{t_B^*} \big(q_y^*(t) - q_y^*(t_d)\big) dt.$$

For $t_B^* - t_d$ sufficiently small, $\Delta B(t_B^*) \leq \underline{B}$, so feasibility is preserved.

Cost differences satisfy, for $t \in (t_d, t_B^*)$,

$$\Delta SC(t) = \int_{q_y^*(t_d)}^{q_y^*(t)} c_y'(q_y)\, dq_y, \qquad \Delta CC(t) = (q_y^*(t) - q_y^*(t_d))(c_v + r\underline{c}_x + m).$$

At t_d, optimality implies

$$c_v + r(\underline{c}_x + \lambda_{B_0} e^{\rho t_d}) + m = u'(q^*(t_d)) = c_y'(q_y^*(t_d)).$$

Since c_y' is increasing and $\lambda_{B_0} > 0$, we have

$$c_y'(q_y) > c_v + r\underline{c}_x + m \quad \text{for all } q_y > q_y^*(t_d),$$

which implies $\Delta CC(t) < \Delta SC(t)$ on (t_d, t_B^*).

Hence the modified path is feasible, yields the same utility, and strictly lowers cost—a contradiction. Therefore any optimal path must satisfy $B(t_B) = 0$. □

A4 Closed-Form Solutions under Quadratic Specifications

To facilitate numerical simulation and analytical characterization, we adopt quadratic functional forms:

$$u(q) = \alpha_u q - \frac{\alpha_u}{2\tilde{q}} q^2,$$
$$c_k(k) = \underline{c}_k k + \frac{\omega}{2} k^2,$$
$$c_y(q_y) = \underline{c}_y q_y + \frac{\xi}{2} q_y^2,$$

where $\underline{c}_k, \underline{c}_y > 0$ denote minimum per-unit costs, $\omega, \xi > 0$ govern convexity, and $\alpha_u, \tilde{q} > 0$ parameterize demand. These forms ensure twice-continuous differentiability and permit closed-form solution of both state and co-state dynamics.

We focus on the case $\bar{K} > K_y$ and $B_0 > B_y$, where the carbon constraint binds and solar experiences temporary displacement. The solution method determines explicit paths

$$\left\{q_x^i(t),\, q_y^i(t),\, q^i(t),\, \lambda_K^i(t)\right\}_{i=1}^{5}$$

across five sub-phases delineated by switching times $\underline{t}_y, t_k, t_\delta, \bar{t}_y, t_B$.

These solutions follow from the Hamiltonian necessary conditions:

$$u'(q_x + q_y) = c_v + r(c_x + \lambda_B e^{\rho t}) + \eta(t) - \gamma_x(t), \tag{AA4.6}$$
$$u'(q_x + q_y) = c_y'(q_y) - \gamma_y(t), \tag{AA4.7}$$
$$\lambda_K(t) = c_k'(k) - \gamma_k(t), \tag{AA4.8}$$
$$\lambda_K(t) K(t) = \gamma_\delta(t), \tag{AA4.9}$$

together with co-state evolution:

$$\dot{\lambda}_B = \rho \lambda_B - \nu_B, \quad \nu_B \geq 0, \quad \nu_B B = 0, \tag{AA4.10}$$
$$\dot{\lambda}_K = (\rho + \delta)\lambda_K + m - \eta - \nu_K, \quad \nu_K \geq 0, \quad \nu_K K = 0, \tag{AA4.11}$$

and complementarity conditions on constraint multipliers $\gamma_x, \gamma_y, \gamma_k, \gamma_\delta, \nu_B, \nu_K$.

A4.1 Expansion Phase: $[0, t_k)$

Sub-phase with active solar: $[0, \underline{t}_y)$**.** No scrapping occurs ($\delta = 0$), so $\dot{K} = k$ and $q_x = K$. Solar remains active ($q_y > 0$, hence $\gamma_y = 0$). The necessary conditions become

$$\alpha_u \left(1 - \frac{K + q_y}{\tilde{q}}\right) = c_v + r(c_x + \lambda_B e^{\rho t}) + \eta, \tag{AA4.12}$$

$$\alpha_u \left(1 - \frac{K + q_y}{\tilde{q}}\right) = \underline{c}_y + \xi q_y, \tag{AA4.13}$$

$$\eta = \rho\lambda_K - \dot{\lambda}_K + m, \tag{AA4.14}$$

$$\lambda_K = \underline{c}_k + \omega k. \tag{AA4.15}$$

From (AA4.15), $k = (\lambda_K - \underline{c}_k)/\omega$, hence $\dot{K} = (\lambda_K - \underline{c}_k)/\omega$ and $\ddot{K} = \dot{\lambda}_K/\omega$. Combining (AA4.12)–(AA4.14) yields

$$\ddot{K} - \rho\dot{K} - \frac{\xi}{\omega\tilde{q}}K = \frac{1}{\omega}\left[\frac{\alpha_u - \underline{c}_y}{2} - c_v - rc_x - m - \rho\underline{c}_k\right] + \frac{r\lambda_B}{\omega}e^{\rho t}.$$

This linear second-order ODE has general solution

$$K(t) = A_1 e^{\mu_1 t} + B_1 e^{\mu_2 t} + \frac{r\tilde{q}\lambda_B}{\xi}e^{\rho t} + \frac{\tilde{q}}{\xi}\left[\frac{\alpha_u - \underline{c}_y}{2} - c_v - rc_x - m - \rho\underline{c}_k\right],$$

$$q_y(t) = \frac{1}{2\xi}\left[-A_1 e^{\mu_1 t} - B_1 e^{\mu_2 t} + \frac{r\tilde{q}\lambda_B}{\tilde{q}}e^{\rho t} + \alpha_u - 2(c_v + rc_x + m + \rho\underline{c}_k)\right],$$

where μ_1, μ_2 are roots of $\mu^2 - \rho\mu - \xi/(\omega\tilde{q}) = 0$:

$$\mu_{1,2} = \frac{\rho \pm \sqrt{\rho^2 + 4\xi/(\omega\tilde{q})}}{2}, \quad \mu_1 > 0,\ \mu_2 < 0.$$

The shadow value follows from differentiation:

$$\lambda_K(t) = \omega\dot{K}(t) + \underline{c}_k = \omega(A_1\mu_1 e^{\mu_1 t} + B_1\mu_2 e^{\mu_2 t} + \rho r\tilde{q}\lambda_B/\xi \cdot e^{\rho t}) + \underline{c}_k.$$

Sub-phase without solar: $[\underline{t}_y, t_k)$**.** Solar production ceases ($q_y = 0$, $\gamma_y > 0$). With $q = K$, the dynamics simplify to

$$\ddot{K} - \rho\dot{K} - \frac{\alpha_u}{\omega\tilde{q}}K = \frac{1}{\omega}\left[\alpha_u - c_v - rc_x - m - \rho\underline{c}_k\right] + \frac{r\lambda_B}{\omega}e^{\rho t},$$

with general solution

$$K(t) = A_2 e^{\nu_1 t} + B_2 e^{\nu_2 t} + \frac{r\tilde{q}\lambda_B}{\alpha_u}e^{\rho t} + \frac{\tilde{q}}{\alpha_u}\left[\alpha_u - c_v - rc_x - m - \rho\underline{c}_k\right],$$

$$\lambda_K(t) = \omega(A_2\nu_1 e^{\nu_1 t} + B_2\nu_2 e^{\nu_2 t} + \rho r\tilde{q}\lambda_B/\alpha_u \cdot e^{\rho t}) + \underline{c}_k,$$

where ν_1, ν_2 solve $\nu^2 - \rho\nu - \alpha_u/(\omega\tilde{q}) = 0$.

Constants A_2, B_2 satisfy continuity at $\underline{t}_y$: $K_2(\underline{t}_y) = K_y$ and $\lambda_{K,2}(\underline{t}_y) = \lambda_{K,1}(\underline{t}_y)$.

A4.2 Stabilization Phase: $[t_k, t_\delta)$

Capacity remains constant: $K(t) = \bar{K}$, $k = \delta = 0$. From (AA4.8), $\lambda_K = \underline{c}_k - \gamma_k$. The co-state equation (AA4.11) with $\nu_K = 0$ (interior capacity) becomes

$$\dot{\gamma}_k = \rho\gamma_k + \eta - m = \rho\gamma_k + \alpha_u\left(1 - \frac{\bar{K}}{\tilde{q}}\right) - c_v - r(c_x + \lambda_B e^{\rho t}) - m.$$

This linear ODE has solution

$$\gamma_k(t) = Ce^{\rho t} - \frac{r\lambda_B}{\rho}(t - t_k)e^{\rho t} - \frac{1}{\rho}\left[\alpha_u\left(1 - \frac{\bar{K}}{\tilde{q}}\right) - c_v - rc_x - m\right]\left(e^{\rho(t-t_k)} - 1\right).$$

Imposing $\gamma_k(t_k) = 0$ (so $\lambda_K(t_k) = \underline{c}_k$) yields $C = 0$, hence

$$\lambda_K(t) = \underline{c}_k + \frac{r\lambda_B}{\rho}(t - t_k)e^{\rho t} + \frac{1}{\rho}\left[\alpha_u\left(1 - \frac{\bar{K}}{\tilde{q}}\right) - c_v - rc_x - m\right]\left(1 - e^{\rho(t-t_k)}\right).$$

A4.3 Hotelling Phase: $[t_\delta, t_B)$

Initial decline: $[t_\delta, \bar{t}_y)$. Capital shadow value vanishes ($\lambda_K = 0$), implying $\eta = m$ and $\gamma_k = \underline{c}_k$. With $q_y = 0$,

$$\alpha_u\left(1 - \frac{K}{\tilde{q}}\right) = c_v + r(c_x + \lambda_B e^{\rho t}) + m,$$

yielding

$$K(t) = \tilde{q}\left[1 - \frac{c_v + rc_x + m}{\alpha_u} - \frac{r\lambda_B}{\alpha_u}e^{\rho t}\right].$$

Final decline with solar revival: $[\bar{t}_y, t_B)$. Both sources operate ($\lambda_K = \gamma_y = 0$). From (AA4.6) and (AA4.7):

$$\alpha_u\left(1 - \frac{K + q_y}{\tilde{q}}\right) = c_v + r(c_x + \lambda_B e^{\rho t}) + m,$$
$$\alpha_u\left(1 - \frac{K + q_y}{\tilde{q}}\right) = \underline{c}_y + \xi q_y.$$

Solving simultaneously:

$$K(t) = \tilde{q}\left[1 + \frac{\underline{c}_y - 2(c_v + rc_x + m)}{\alpha_u} - \frac{2r\lambda_B}{\alpha_u}e^{\rho t}\right],$$
$$q_y(t) = \frac{\tilde{q}}{\xi}\left[\frac{\alpha_u - \underline{c}_y}{2} - c_v - r(c_x + \lambda_B e^{\rho t}) - m\right].$$

A4.4 Carbon Budget Constraint

The cumulative emissions constraint requires

$$B_0 = \zeta r \int_0^{t_B} K(t)\,dt = \zeta r \left[\sum_{i=1}^{5} \int_{t_{i-1}}^{t_i} K_i(t)\,dt \right],$$

where $t_0 = 0, t_1 = \underline{t}_y, t_2 = t_k, t_3 = t_\delta, t_4 = \bar{t}_y, t_5 = t_B$ denote phase boundaries. Substituting the closed-form solutions and integrating yields a transcendental equation in the unknown parameters $\{\lambda_B, A_1, B_1, A_2, B_2, \bar{K}, \underline{t}_y, t_k, t_\delta, \bar{t}_y, t_B\}$, which can be solved numerically given boundary conditions.

A4.5 Boundary Conditions

The following 12 conditions determine the unknowns:

1. $K(0) = 0$ (initial capital stock)
2. $K_1(\underline{t}_y) = K_y$ (solar displacement threshold)
3. $K_2(\underline{t}_y) = K_1(\underline{t}_y)$ (continuity at first switching)
4. $\lambda_{K,2}(\underline{t}_y) = \lambda_{K,1}(\underline{t}_y)$ (co-state continuity)
5. $\dot{K}_2(t_k) = 0$ (investment ceases)
6. $K_2(t_k) = \bar{K}$ (peak capacity definition)
7. $\lambda_K(t_k) = \underline{c}_k$ (marginal investment cost)
8. $\lambda_K(t_\delta) = 0$ (scrapping begins)
9. $K_3(t_\delta) = K_4(t_\delta)$ (continuity at scrapping threshold)
10. $K_4(\bar{t}_y) = K_y$ (solar revival threshold)
11. $K_5(t_B) = 0$ (complete fossil phase-out)
12. $B_0 = \zeta r \int_0^{t_B} K(t)\,dt$ (budget exhaustion)

These form a system of nonlinear equations solvable via Newton-Raphson or shooting methods, yielding the complete optimal path characterized in Section **??**.